 doi:10.1111/j.1365-2958.2010.07062.x

Epigenetic mechanisms regulate stage differentiation in the minimized protozoan *Giardia lamblia*

Sabrina Sonda,[1*†] Laura Morf,[1†] Iveta Bottova,[1] Hansruedi Baetschmann,[2] Hubert Rehrauer,[2] Amedeo Caflisch,[3] Mohamed-Ali Hakimi[4] and Adrian B. Hehl[1]**

[1]*Institute of Parasitology and* [3]*Department of Biochemistry, University of Zürich, 8057 Zürich, Switzerland.*

[2]*Functional Genomics Center Zürich, 8057 Zürich, Switzerland.*

[4]*UMR5163, Laboratoire Adaptation et Pathogénie des Micro-organismes, Centre National de la Recherche Scientifique (CNRS), Université Joseph Fourier Grenoble 1, BP 170, 38042 Grenoble, Cedex 09, France.*

Summary

Histone modification is an important mechanism regulating both gene expression and the establishment and maintenance of cellular phenotypes during development. Regulation of histone acetylation via histone acetylases and deacetylases (HDACs) appears to be particularly crucial in determining gene expression patterns. In this study we explored the effect of HDAC inhibition on the life cycle of the human pathogen *Giardia lamblia*, a highly reduced parasitic protozoan characterized by minimized cellular processes. We found that the HDAC inhibitor FR235222 increased the level of histone acetylation and induced transcriptional regulation of ~2% of genes in proliferating and encysting parasites. In addition, our analyses showed that the levels of histone acetylation decreased during differentiation into cysts, the infective stage of the parasite. Importantly, FR235222 treatment during encystation reversed this histone hypo-acetylation and potently blocked the formation of cysts. These results provide the first direct evidence for epigenetic regulation of gene expression in this simple eukaryote. This suggests that regulation of histone acetylation is involved in the control of *Giardia* stage differentiation, and identifies epigenetic mechanisms as a promising target to prevent *Giardia* transmission.

Accepted 17 January, 2010. For correspondence. *E-mail sabrina.sonda@vetparas.uzh.ch; Tel. +41 44 635 85 14; Fax +41 44 635 89 07; **E-mail adrian.hehl@access.uzh.ch; Tel. +41 44 635 85 26; Fax +41 44 635 89 07. †These authors contributed equally to this work.

Introduction

Regulation of gene expression is a complex process controlled by several molecular mechanisms including modification of chromatin structure, activity of sequence-specific DNA binding proteins, and post-transcriptional modulation of mRNA levels. Epigenetic histone modifications result in alteration of chromatin structure, which in turn induces changes in gene expression (reviewed in Jenuwein and Allis, 2001; Kouzarides, 2007). In general terms, the process of covalent histone acetylation regulates gene expression by modifying DNA packaging, with histone hyperacetylation leading to chromatin decondensation and activation of transcription. Conversely, histone hypoacetylation leads to a tighter DNA-histone binding, with consequent chromatin condensation and gene silencing. The level of histone acetylation is strictly controlled by the concerted activity of histone acetylases (HATs) and deacetylases (HDACs), which act as central organizers of chromatin remodelling and gene transcription. The correct regulation of HDACs is critical for cellular homeostasis. The importance of a tight control of HDAC activity is exemplified by its upregulation associated with uncontrolled cell growth at the onset of cancer (Glozak and Seto, 2007). In this context, considerable efforts have been invested to develop inhibitors of HDAC activity (HDACi) as anti-cancer drugs, as HDACi were shown to counteract aberrant cell cycle regulation in cancer cells both *in vitro* and *in vivo* (Bolden *et al.*, 2006). In addition, recent studies revealed that the activity of HDACs is crucial not only for cell cycle regulation but also for the orchestration of development and cell differentiation in different mammalian organs (Margueron *et al.*, 2005; Haumaitre *et al.*, 2009). Despite these recent advances, our understanding of the roles HDACs play remains limited.

In this study we investigated whether HDAC activity also plays a role in the differentiation process of the intestinal pathogenic parasite *Giardia lamblia*, a protozoan characterized by a highly reduced genome and significant minimization of most cellular systems due to secondary

reduction (Morrison *et al.*, 2007). In this respect, the parasite is a useful model organism to study basic biological processes of higher eukaryotes. The *G. lamblia* life cycle is comprised of highly motile flagellated trophozoites and quiescent cyst surrounded by a protective cyst wall (Gerwig *et al.*, 2002). Differentiation from the trophozoite to the cyst stage is critical for the parasite survival in the environment and for disease transmission.

Giardia lamblia encystation is a complex process that involves both expression of specific proteins and also changes in the parasite's metabolism (Adam, 2001). The encystation process begins with an early phase where cyst wall components, including cyst wall proteins (CWPs) 1–3, are synthesized and accumulated in encystation-specific secretory vesicles (ESVs). ESVs are formed transiently only during the time of encystation and display Golgi-like characteristics (Lujan *et al.*, 1998; Marti and Hehl, 2003; Hehl and Marti, 2004; Stefanic *et al.*, 2009), allowing both maturation and export of the CWPs to the cell exterior to form the cyst wall. This late phase is completed with the sequential secretion of two fractions of cyst wall material to the parasite surface 20–24 h after induction of encystation, where it polymerizes to a rigid extracellular matrix, the cyst wall.

Despite recent discoveries in the field of *G. lamblia* encystation, our understanding of the molecular mechanisms initiating and regulating gene expression during this critical process remains incomplete. Several factors have been implicated, including kinase and phosphatase-mediated signal transduction (Ellis *et al.*, 2003; Bazan-tejeda *et al.*, 2007; Lauwaet *et al.*, 2007; Pan *et al.*, 2009), arginine deiminase activity (Touz *et al.*, 2008), proteinases (Touz *et al.*, 2002a) and dipeptidyl peptidase IV (Touz *et al.*, 2002b). In addition, we recently showed that the synthesis of the sphingolipid glucosylceramide is also essential for complete cyst formation in *G. lamblia* (Stefanic *et al.*, 2009). However, much less is known about transcriptional regulation of encystation-specific genes. To date only a few putative encystation-related transcription factors have been identified and partially characterized in *G. lamblia*: a Myb2 homologue (Sun *et al.*, 2002; Huang *et al.*, 2008), two members of the GARP family (Sun *et al.*, 2006), one ARID family member (Wang *et al.*, 2007) and a recently described WRKY protein (Pan *et al.*, 2009). All these transcription factors, whose expression increases during encystation, bind to the short promoter of encystation-induced genes and act as *trans*-activators of transcription. In addition to *trans*-activating factors, mechanisms for negative regulation have also been suggested to control CWP expression in vegetative trophozoites, including regulation of mRNA stability via the 3′ untranslated region (UTR) (Hehl *et al.*, 2000), the nonsense-mediated mRNA decay (NMD) factor UPF1 (Chen *et al.*, 2008), and presence of negative *cis*-acting elements in the CWP promoters (Davis-Hayman *et al.*, 2003).

Because *G. lamblia* encystation is associated with clearly detectable changes in mRNA levels and the degree of histone acetylation is critical for transcriptional control, we hypothesized that epigenetic chromatin modifications via histone acetylation may participate in the modulation of stage differentiation in this parasite. To test this, we analysed whether modifying histone acetylation levels by inhibiting giardial HDAC affected parasite encystation.

Results

Histone acetylation decreases during G. lamblia *stage conversion*

Giardia lamblia encystation is regulated at the transcriptional level and results in high levels of transcription of encystation-specific genes during the first 7–9 h post induction. To investigate whether epigenetic mechanisms dependent on histone acetylation are involved in the stage conversion of *G. lamblia*, we compared the histone acetylation levels in trophozoites and encysting cells. To test this, we incubated isolated parasites with an anti-acetyl lysine antibody after chemical fixation and detergent permeabilization. Immunofluorescence analysis revealed that the labelling was restricted to the nuclei and that it overlapped with DAPI-stained DNA, as expected for labelled histones (Fig. 1A). As previously shown for the labelling of methyl-modified histones (Dawson *et al.*, 2007), the two giardial nuclei were similarly stained, indicating that the chromatin of both nuclei can be modified by the acetylation mark. Importantly, no cross-reaction was observed with cytosolic acetylated proteins, including tubulin (Fig. 4B), indicating that the antibody exclusively recognizes acetylated proteins restricted to the nucleus.

Next we quantified the degree of histone acetylation in trophozoites and encysting cells by flow cytometry. Our analysis showed that the staining intensity decreased in differentiating trophozoites (Fig. 1B), suggesting that the levels of histone acetylation are regulated in the parasite in a stage-specific manner.

Characterization of G. lamblia *HDAC*

As the cellular levels of histone acetylation are maintained by the concerted activity of HAT and HDAC enzymes, we investigated whether these enzymes are present in the parasite.

Analysis of the *Giardia* Genome Database (http://giardiadb.org) revealed the presence of putative enzymes responsible for histone modification, including HDACs (Table 1). In mammalian cells, the classical HDAC family consists of the ubiquitously expressed class I (HDACs 1–3, 8) and the tissue-specific classes II (HDACs 4–7, 9,

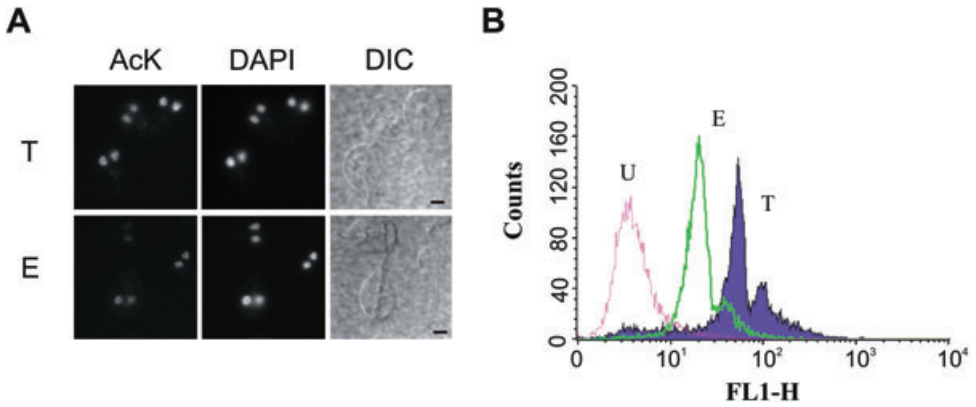

Fig. 1. Acetylation levels decrease in *G. lamblia* upon induction of encystation. Trophozoites (T) and parasites induced to encyst for 16 h (E) were probed for acetylated lysine (AcK).
A. Immunofluorescence analysis showing the staining restricted to the nuclei in both stages of the parasite. DAPI, nuclear staining; DIC, differential interference contrast. Scale bar: 3 μm.
B. Overlay histogram of the FACS analysis showing trophozoites (T) and encysting cells (E) stained for AcK. U, unstained cells. Note the decreased intensity of AcK staining in encysting cells compared with trophozoites (logarithmic scale on *x*-axis).

10) and IV (HDAC11), while the structurally unrelated class III is composed of sirtuin proteins 1–7. Interestingly, the *G. lamblia* genome codes for only one predicted homologue of the classical HDAC family, and four additional predicted sirtuin type 2 family homologues.

Multiple sequence alignments showed a high level of similarity between the single giardial HDAC and orthologues of protozoan and metazoan species (Fig. 2 and Table 2), indicating that the protein is highly conserved in this parasite. Importantly, the amino acids thought to be critical for human HDAC1 activity, including the residues in the catalytic pocket that co-ordinate binding to the co-factor Zn^{2+} and that are in contact with the HDACi Trichostatin A (TSA) (Finnin *et al.*, 1999; Vannini *et al.*, 2004), are also present in the giardial HDAC. Interestingly, the predicted giardial HDAC does not possess an AT insertion which is typical of Apicomplexa (Bougdour *et al.*, 2009), but contains a unique four-residue insertion in position 283–286, which is not found in other species.

Table 1. Putative histone modifying enzymes in *G. lamblia*.

Histone acetylases	
GL50803_10666	Histone acetyltransferase GCN5
GL50803_2851	Histone acetyltransferase MYST2
GL50803_16639	Histone acetyltransferase Elp3
GL50803_14753	Histone acetyltransferase type B subunit 2
GL50803_17263	Histone acetyltransferase MYST1
Histone deacetylases	
GL50803_3281	Histone deacetylase I
GL50803_10707	NAD-dependent histone deacetylase Sir2
GL50803_10708	Hypothetical protein, Sir2 domain
GL50803_16569	Transcriptional regulator, Sir2 family
GL50803_6942	Sir2 family protein
GL50803_11676	Sirtuin type 2
Histone methylases	
GL50803_8921	Set-2, putative
GL50803_13838	Hypothetical protein
GL50803_13790	Hypothetical protein
GL50803_9130	Histone methyltransferase HMT1
GL50803_17036	Hypothetical protein
GL50803_221691	Histone methyltransferase HMT2

To analyse the localization of giardial HDAC, a recombinant variant fused to a C-terminal HA tag was expressed in the parasites. Immunofluorescence analysis of transgenic cells revealed that the protein localizes to the parasite nuclei, suggesting that the giardial HDAC is likely to function in this subcellular location (Fig. 3A).

To gain further insights into the structure-function basis of giardial HDAC, a homology model was generated using the recently resolved structure of human HDAC8 as a template (Fig. 3B) (Vannini *et al.*, 2007). The predicted 3D structure revealed a striking similarity with the human homologue. In addition, position and orientation of the active site residues are essentially identical in the giardial and human structures, further supporting the predicted catalytic activity of *G. lamblia* HDAC.

To investigate whether the catalytic pocket of giardial HDAC could accommodate HDACi, we modelled the structure of the protein in complex with the cyclic tetrapeptide FR235222 (Mori *et al.*, 2003), a potent inhibitor that was recently shown to specifically target HDAC3 in the Apicomplexan parasite *Toxoplasma gondii* (Bougdour *et al.*, 2009) (Fig. 3C). The 3D structure of FR235222 was built using the values of the backbone dihedral angles as they are in the NMR solution conformation (Rodriquez *et al.*, 2006). Three binding modes of FR235222 in the homology model of *G. lamblia* HDAC were generated by docking using the program WITNOTP (Armin Widmer, Novartis Pharma, Basel, Switzerland). In all binding modes, the long side-chain of FR235222 was positioned in the deep pocket of HDAC with the ketone moiety at the tip of the side-chain

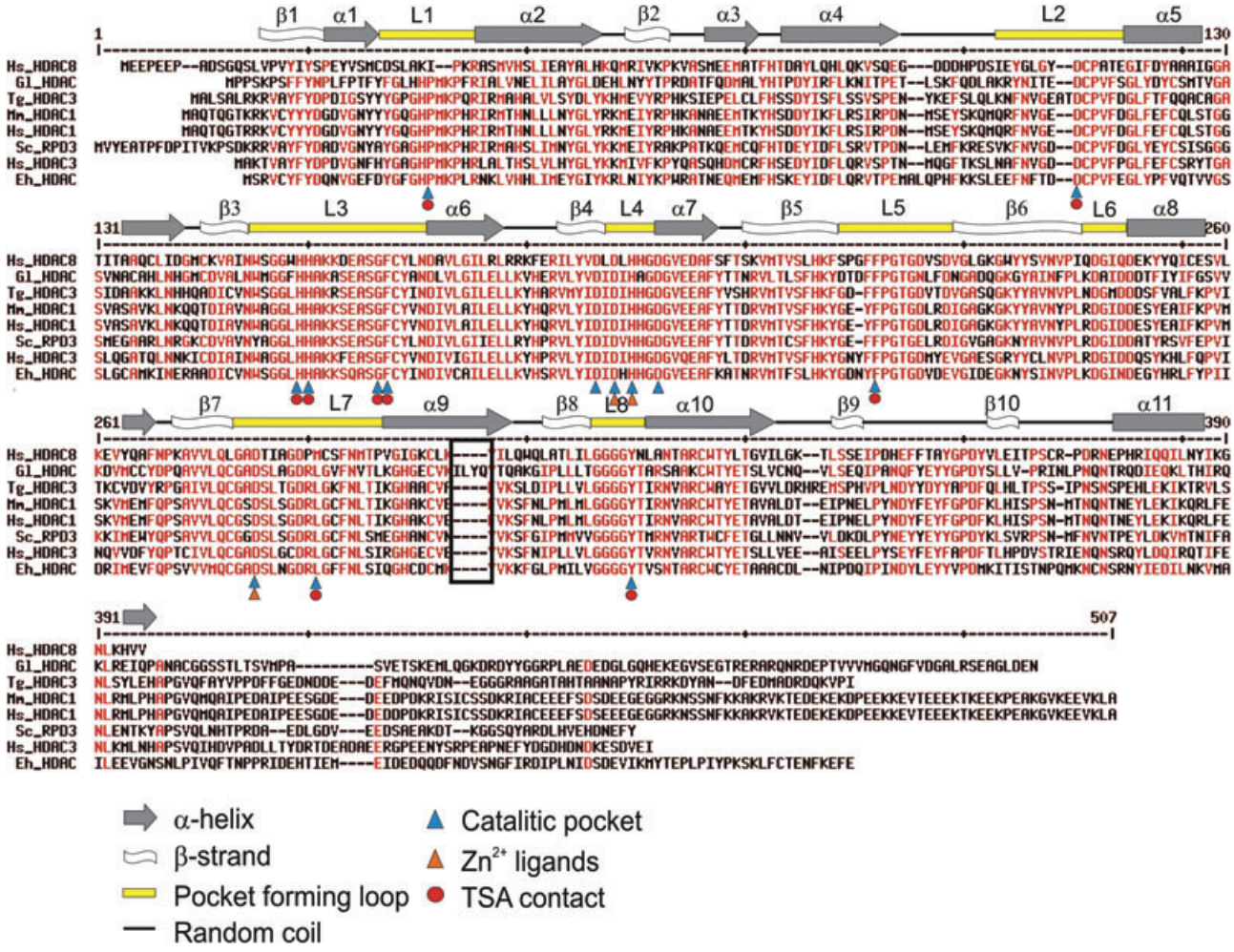

Fig. 2. Multiple protein sequence alignment of giardial HDAC with selected orthologues. Indicated are the residues important for catalytic activity and involved in zinc and TSA binding, based on crystal structure of related HDAC (Finnin *et al.*, 1999; Vannini *et al.*, 2004). The four residues of the *G. lamblia*-specific insertion are boxed. Alignments were performed with Multalin (http://bioinfo.genotoul.fr/multalin/). Gene bank accession numbers: GlHDAC (AAU89077), TgHDAC3 (AAY53803; ToxoDB accession no. 42.m00014), EhHDAC (AAV33348), HsHDAC1 (CAG46518), HsHDAC3 (NP_003874.2), HsHDAC8 (AF245664), MsHDAC1 (AAI08372), ScRPD3 (AAB20328).

Table 2. Sequence comparison of Gl HDAC with selected orthologues.

Name	Identity (%)	Similarity (%)	AA overlap
Tg_HDAC3	48	68	376
Eh_HDAC	46	64	377
Mm_HDAC1	50	72	368
Hs_HDAC1	50	72	368
Sc_RPD3	51	69	372
Hs_HDAC3	45	66	432
Hs_HDAC8	41	62	368

G. lamblia, GlHDAC (AAU89077); *T. gondii* TgHDAC3 (AAY53803); *E. hystolitica*, EhHDAC (AAV33348); *H. sapiens*, HsHDAC1 (CAG46518); HsHDAC3 (NP_003874.2); HsHDAC8 (AF245664); *M. musculus*, MsHDAC1 (AAI08372); *S. cerevisiae*, ScRPD3 (AAB20328).

chelating the zinc. The three binding modes differ from each other in the orientations of the phenylalanine, isovaline, and 4-methyl-proline side-chains on the rim of the deep pocket. Each binding mode was energy minimized with rigid protein and zinc atom using the TAFF force field (Clark *et al.*, 1989). Upon energy minimization there is good surface complementarity in all of the three binding modes. Furthermore, the binding energy is similar in the three minimized structures, which is consistent with the heterogeneity of orientations observed for a set of inhibitors of human HDAC8 (Dowling *et al.*, 2008).

Inhibition of HDAC increases histone acetylation levels in G. lamblia

Because the stage conversion of *G. lamblia* correlated with decreased levels of histone acetylation, we investi-

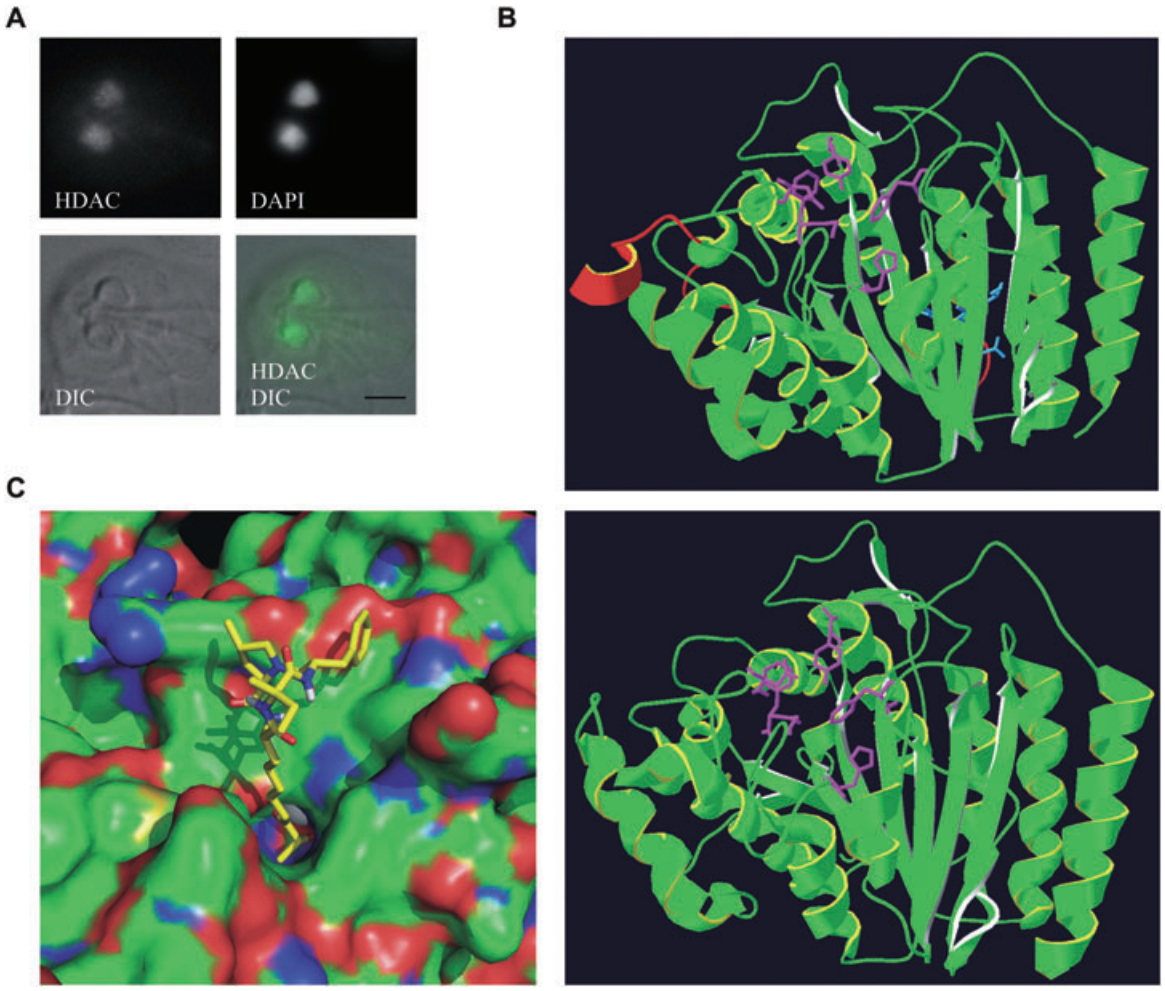

Fig. 3. Characterization of *G. lamblia* HDAC.
A. Fluorescence analysis of parasites expressing recombinant giardial HDAC fused to a C-terminal HA tag and encysted for 16 h. Cells were co-stained for nuclei (DAPI). DIC, differential interference contrast image. Scale bars: 3 μm.
B. 3D homology model of GlHDAC (upper panel) built with the SWISS-MODEL program and X-ray structure of HsHDAC8 (lower panel) used as a template. Key residues of the active-site are violet (Asp 101, His 142, Phe 152, Phe 208, Tyr 306 in HsHDAC8; Asp 94, His 135, Phe 145, Phe 201, Tyr 303 in GlHDAC). The four amino acids of GlHDAC insertion are blue. The GlHDAC region not covered by the HsHDAC8 template is red.
C. Predicted binding mode of FR235222 (sticks) in the homology model of GlHDAC (surface rendering). The energy minimization was performed with rigid protein. The atoms of FR235222 are coloured according to atomic element with carbon in yellow, nitrogen in blue, oxygen in red, and hydrogen in grey. Hydrogen atoms on the side-chains are not shown to avoid overcrowding. The polar surface of HDAC is coloured according to atomic element (nitrogen in blue and oxygen in red) while the non-polar surface is green. The zinc atom is the white sphere that is visible only partially at the bottom of the deep pocket close to the centre of the image. The long side-chain of FR235222 fits nicely in the cavity, and the two oxygen atoms at its tip chelate the zinc atom. Figure prepared with the program PyMOL (DeLano Scientific, USA).

gated whether reversing the decrease in acetylation by inhibiting HDAC could prevent parasite encystation. To this aim, we tested in the parasite the inhibitory activity of FR235222, the potent HDACi which was predicted to fit in the active site of *G. lamblia* HDAC in our 3D model. Immunofluorescence and quantitative analysis by flow cytometry revealed that treatment with FR235222 increased acetylation levels in encysting parasites (Fig. 4A). Selected subtypes of HDACs have been shown to target cytosolic non-histone proteins, including tubulin (Schemies *et al.*, 2009). In our experiments, FR235222 treatment did not increase the acetylation levels of tubulin (Fig. 4B), implying not only that the inhibitor is not affecting the activity of other cellular deacetylases in a non-specific manner, but also that the single giardial HDAC is likely not able to accept tubulin as a substrate. In addition, nuclear basic proteins were isolated by acid extraction and probed for acetylation (Fig. 4C). Distinct acetylated proteins were identifiable in the region of 11–16 kDa, corresponding with the predicted masses of histone proteins in *Giardia* (Triana *et al.*, 2001). Importantly, their acetylation level specifically increased in the presence of

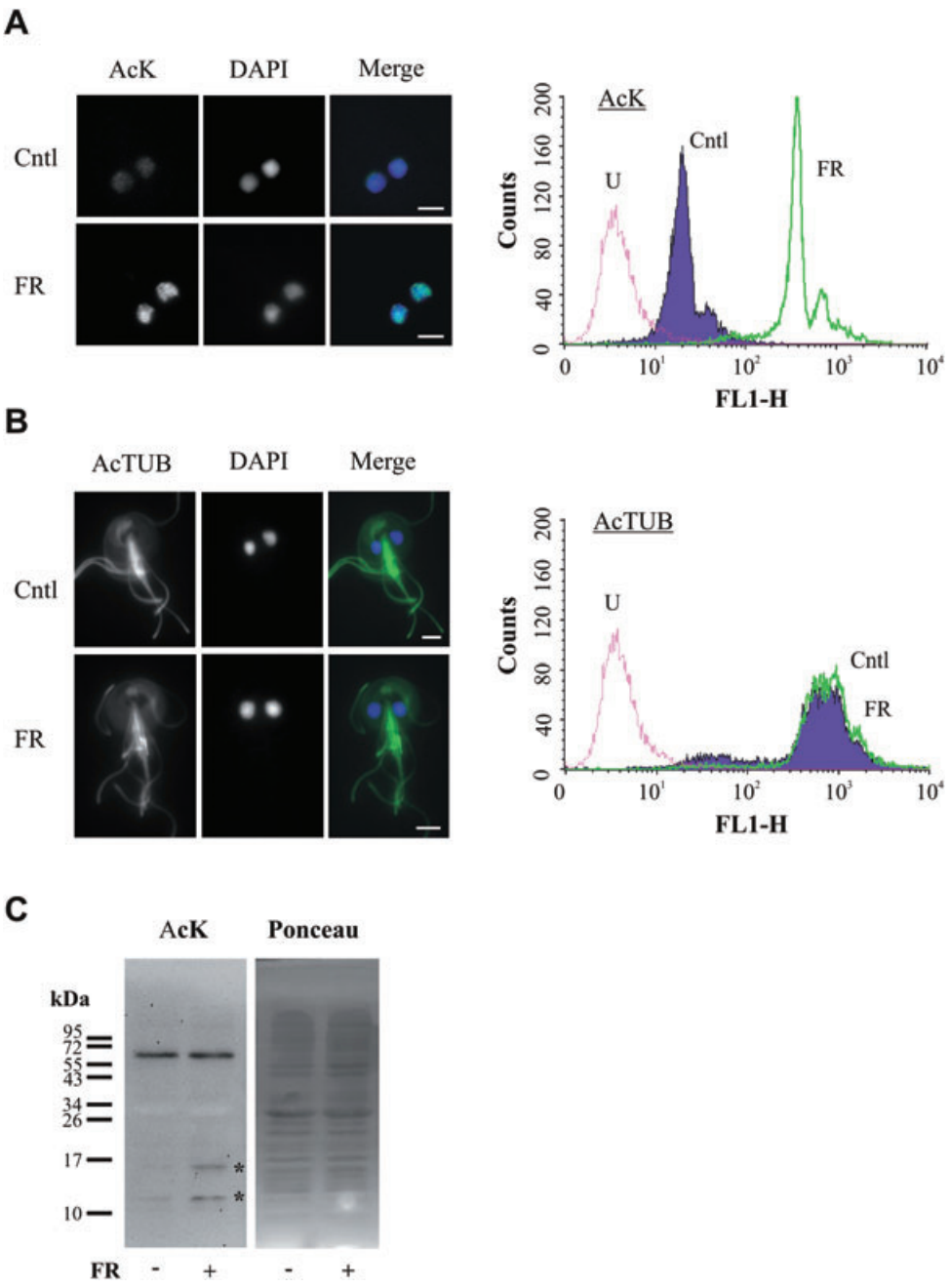

Fig. 4. FR235222 treatment increases acetylation levels of encysting cells.
A and B. Encysting parasites were treated with 2 μM FR235222 (FR) or solvent (Cntl), as described. Cells were analysed by immunofluorescence (left panels) after staining with anti-acetylated lysine (AcK) (A) or anti-acetylated tubulin (AcTUB) antibodies (B). DAPI, nuclear staining. Scale bar: 3 μm. The level of AcK and AcTUB upon FR235222 treatment was quantified by flow cytometry (right panels). Overlay histograms showing cells unstained (U), treated with solvent (Cntl) or 2 μM FR235222 (FR). Note the increased AcK signal in presence of the drug.
C. Encysting cells were treated with 2 μM FR235222 (FR) or solvent. Aliquots of 16 μg of acid-extracted proteins were separated by SDS-PAGE and probed with anti-acetylated lysine antibody. Note the increased acetylation of proteins with the predicted mass of giardial histones (asterisks) in presence of the HDAC inhibitor.

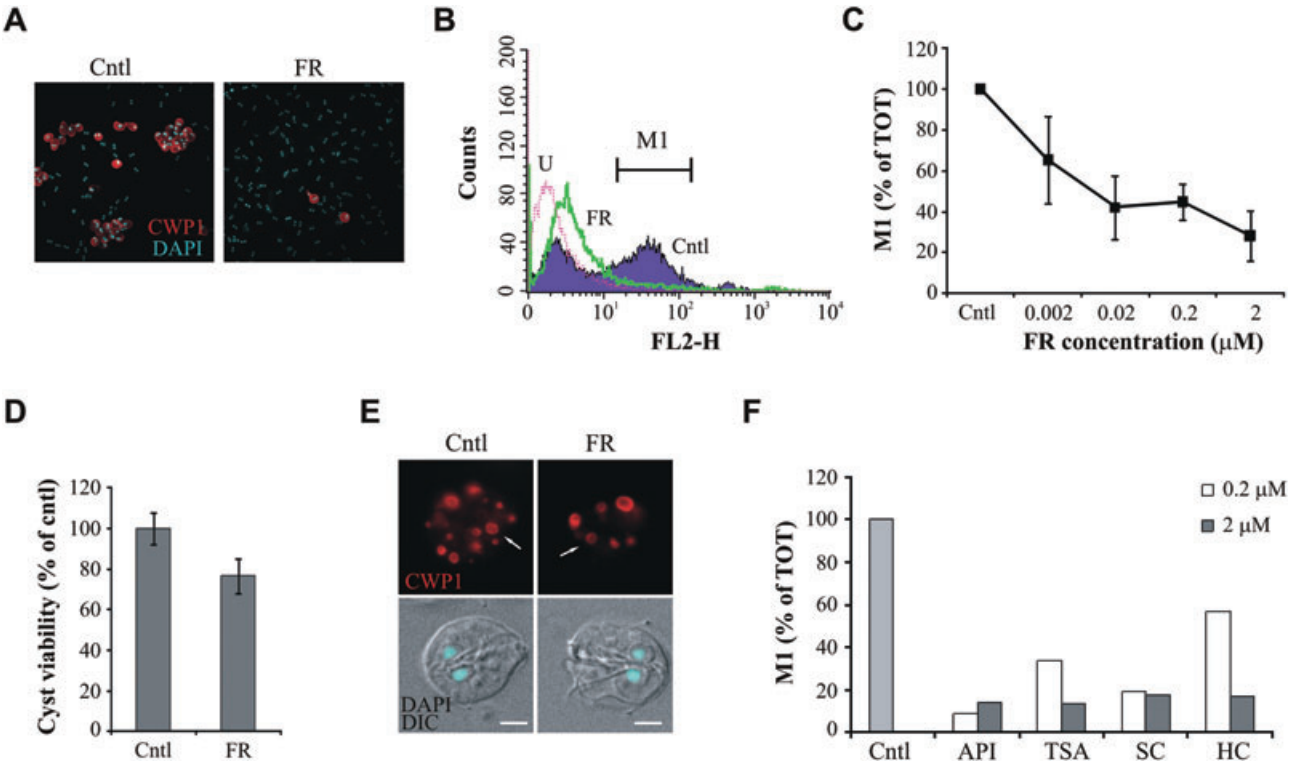

Fig. 5. FR235222 treatment inhibits *G. lamblia* encystation.
A. Encysting parasites were treated for 24 h with 2 μM FR235222, as described in the *Experimental procedures* section. Cells were stained with anti-cyst wall protein 1 (CWP1) antibody without permeabilization and analysed by immunofluorescence. Note the decreased number of cysts in the treated sample. DAPI, nuclear staining.
B. Encysting parasites were treated as in (A), permeabilized and stained for CWP1 followed by flow cytometry quantification. Overlay histogram showing cells unstained (U), treated with solvent (Cntl) or 2 μM FR235222 (FR).
C. Encysting parasites were treated with the indicated concentrations of FR235222 (FR) or solvent (Cntl), stained for CWP1 after permeabilization and analysed by flow cytometry. The amount of cells with M1 fluorescence is expressed as percentage of total cell number (TOT). Note the dose-dependent decrease in CWP1 expression upon drug treatment.
D. Viability of cysts following drug treatment was tested by trypan blue exclusion. Results of a representative experiment are presented as percentage of control ± standard errors ($n = 3$).
E. Immunofluorescence analysis of treated parasites as in (B). Note the normal morphology of encystation-specific vesicles (ESV, arrow) containing CWP1 in both treated and control samples. DAPI, nuclear staining; DIC, differential interference contrast. Scale bar: 3 μm.
F. Encysting parasites were treated with the indicated concentrations of HDAC inhibitors apicidin (API), Trichostatin A (TSA), scripaid (SC) and HC-toxin (HC) and CWP1 expression was quantified by flow cytometry after permeabilization. The amount of cells with M1 fluorescence is expressed as percentage of total cell number (TOT). The analysis revealed that all the compounds tested inhibited the expression of CWP1.

FR235222. Histone identities of the bands in the 11–16 kDa region were further confirmed by mass spectrometry analysis (Fig. S1).

Collectively, our data provide strong evidence that treatment with the HDACi FR235222 induced histone hyperacetylation in the parasite.

FR235222 inhibits expression of cyst wall proteins in encysting G. lamblia

Having shown that FR235222 treatment induces histone hyper-acetylation in *G. lamblia*, we next evaluated whether increased acetylation levels prevented parasite stage conversion to cysts. Induction of encystation results in high levels of expression of the main structural CWPs. Immunofluorescence analysis of CWP1 expression in induced cultures revealed a considerably decreased number of cysts in the inhibitor-treated sample compared with control cells (Fig. 5A). In addition, the few cysts produced in presence of FR235222 were less viable than the control sample (Fig. 5D). To determine whether the low number of cysts was due to a reduced CWP1 expression or a defect of protein secretion and consequent accumulation in the cell interior, we quantified the protein expression in detergent-permeabilized cells. Population-wide analysis by flow cytometry showed that FR235222 severely impaired expression of CWP1 (Fig. 5B). Interestingly, while the maximal inhibition of CWP1 expression was obtained by pre-treating the cells with FR235222 prior to induction of encystation, a substantial decrease of

CWP1 protein level was also observed in the absence of drug pre-treatment, indicating a rapid effect of the inhibitor on CWP1 synthesis (Fig. S2).

Next, we performed a dose–response analysis to determine the potency of the FR235222-mediated inhibition of *G. lamblia* encystation. Flow cytometry quantification revealed that FR235222 was effective in inhibiting CWP1 expression already at low nanomolar concentration (Fig. 5C).

In addition, we tested whether FR235222 treatment not only inhibited CWP1 expression, but also altered the protein's intracellular distribution, a phenotype we recently described when parasite encystation was blocked following inhibition of sphingolipid synthesis (Štefanić *et al.*, submitted). Immunofluorescence analysis of encysting parasites showed that both in control cells and in the minor proportion of FR235222-treated cells with detectable CWP1 levels, the protein was mainly localized in ESVs with typical morphology, indicating that formation of these compartments was not compromised (Fig. 5E).

To further confirm that the FR235222 inhibition of *G. lambia* encystation was indeed a specific effect, additional known HDACi, i.e. apicidin, TSA, scripaid and HC-toxin, were tested. All the inhibitors were highly effective in reducing CWP1 expression, as assessed by flow cytometry analysis (Fig. 5F) and enumeration of CWP1-expressing parasites by manual counting (Fig. S4). Collectively, our data indicate that exposure of encysting cells to HDACi severely compromised the encystation process by preventing induction of CWP expression.

FR235222 treatment does not downregulate the expression of constitutively expressed proteins

Next we asked whether FR235222-mediated downregulation of protein expression took place at a global level or it was specific for encystation-induced protein. We tested this by quantifying the degree of regulation of constitutively expressed proteins. The cellular levels of three unrelated endogenous proteins [namely the small GTPase Sar1, the endoplasmic reticulum-resident protein disulphide isomerase 2 (PDI2) and clathrin], which are involved in the secretory transport of CWP protein but whose expression is not stage-regulated, were monitored in encysting cells treated with FR235222. Flow cytometry quantification using antibodies against these three proteins revealed that none of them decreased in presence of the inhibitor (Fig. 6A), indicating that HDAC targeting does not result in a general reduction of protein expression.

We next tested whether the elements responsive to FR235222 regulation were located in the non-coding flanking regions of CWP1. To do this, 120 nucleotides of CWP1 5′ UTR flanking region containing the CWP1 promoter (Hehl *et al.*, 2000) were cloned in front of recombinant Sar1 fused to a N-terminal HA tag as a reporter, followed by 180 nucleotides of 3′ sequence flanking the CWP1 ORF, containing the poly A addition site (Fig. 6B). Transgenic parasites were obtained by stable integration of the construct into the parasite genome. Similar to the observed inhibition of endogenous CWP1, FR235222 treatment downregulated the expression of the Sar1-HA reporter in engineered parasites (Fig. 6C, D). Drug-mediated inhibition of Sar1-HA expression was also observed in parasites transiently transfected with an analogous construct, which was maintained episomaly (not shown). These results show that the short regions flanking the CWP1 ORF and containing all elements necessary for stage-regulated expression of CWP1 were sufficient for preventing CWP1 induction in response to FR235222 treatment.

FR235222 does not inhibit G. lamblia *replication*

FR235222 treatment was shown to efficiently block the replication of Apicomplexan parasites with an EC_{50} of 10 nM (Bougdour *et al.*, 2009). Interestingly, when *G. lamblia* were incubated with FR235222 up to 2 μM, no reduction of replication was observed in encysting parasites and only a modest inhibition in trophozoite cultures (Fig. 7A). This result indicates that the increased levels of histone acetylation induced by FR235222 were not caused by toxicity or dying parasites. Next we tested the sensitivity of the parasite to other HDACi. Neither treatment with apicidin nor with scripaid or HC-toxin up to 2 μM affected parasite replication (data not shown). In contrast, treatment with TSA severely inhibited replication of both parasite stages at nanomolar concentrations; as TSA is a broad range inhibitor of cellular deacetylases (Blagosklonny *et al.*, 2002), it is conceivable that the block of replication is due to a non-specific activity towards other essential proteins. Taken together, these results show that treatment with HDACi, which are known to affect replication in other species, often did not have the same inhibitory effect on *G. lamblia* replication.

Given the close association of *Giardia* with the hosts' intestinal epithelial cells, we tested whether FR235222 was detrimental for mammalian cells. Four intestinal and fibroblast cell lines were grown to sub-confluence (Fig. 7B) or confluence (not shown), exposed to the drug, and their metabolic activity was quantified as a measure of cell viability. At both confluencies, 24 h of treatment with 0.02 μM FR235222 (a concentration which blocks *G. lamblia* encystation) did not affect metabolic activity of the intestinal cells and only moderately reduced the activity in the fibroblasts. Higher inhibitor concentrations up to 2 μM

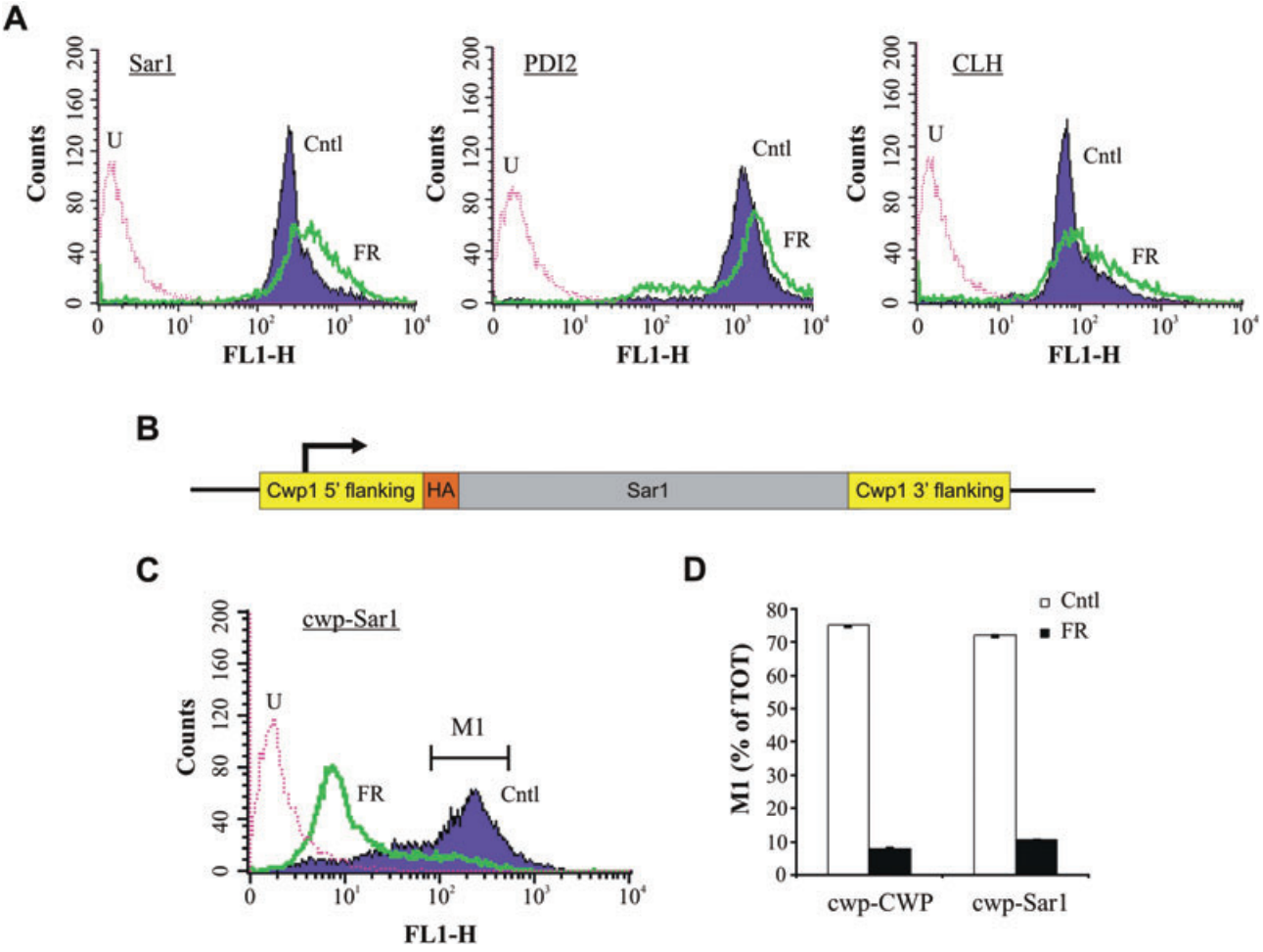

Fig. 6. FR235222 treatment does not reduce the expression of constitutive proteins.
A. Encysting parasites were treated for 24 h with FR235222, as described. Flow cytometry quantification of Sar1, protein disulphide isomerase 2 (PDI2) and clathrin (CLH) showed that the protein expression did not decrease upon inhibitor treatment. Overlay histograms showing cells unstained (U), treated with solvent (Cntl) or 2 μM FR235222 (FR).
B. Schematic representation of Sar1-HA construct.
C. Engineered parasites expressing Sar1-HA under control of CWP1 promoter were treated as in (A), stained for recombinant Sar1 using an anti-HA antibody and quantified by flow cytometry. Overlay histogram showing cells unstained (U), treated with solvent (Cntl) or 2 μM FR235222 (FR).
D. The same engineered parasites were additionally probed for endogenous CWP1 expression. The amount of cells with M1 fluorescence is expressed as percentage of total cell number (TOT). Note the decreased expression of both proteins upon inhibitor treatment.

induced different responses in different cell types, ranging from no alteration in viability in Caco-2 cells to 50% inhibition in fibroblasts. Moreover, inhibitor-mediated toxicity was not induced during co-culture of intestinal cells with *G. lamblia* (Fig. S3). These results indicate that FR235222 treatment at concentrations inhibitory for *G. lamblia* encystation did not reduce the viability of mammalian intestinal cells.

FR235222 treatment of trophozoites does not induce stage conversion

Our findings revealed that increasing the levels of histone acetylation with FR235222 treatment during encystation blocked stage differentiation in *G. lamblia*. To further investigate the hypothesis that acetylation must decrease to allow differentiation, we evaluated whether pharmacologically increased acetylation in trophozoites would keep the cells at the trophozoite stage or induce parasite differentiation. FR235222 incubation increased histone acetylation in trophozoites (Fig. 7C, left panel), although not as potently as in encysting cells (Fig. 4A). Importantly, the degree of tubulin acetylation did not change in the presence of the drug (Fig. 7C, right panel), indicating that FR235222 was effective in specifically modulating the histone acetylation levels in both life stages of the parasite. To test whether HDAC inhibition in trophozoites induced parasite stage

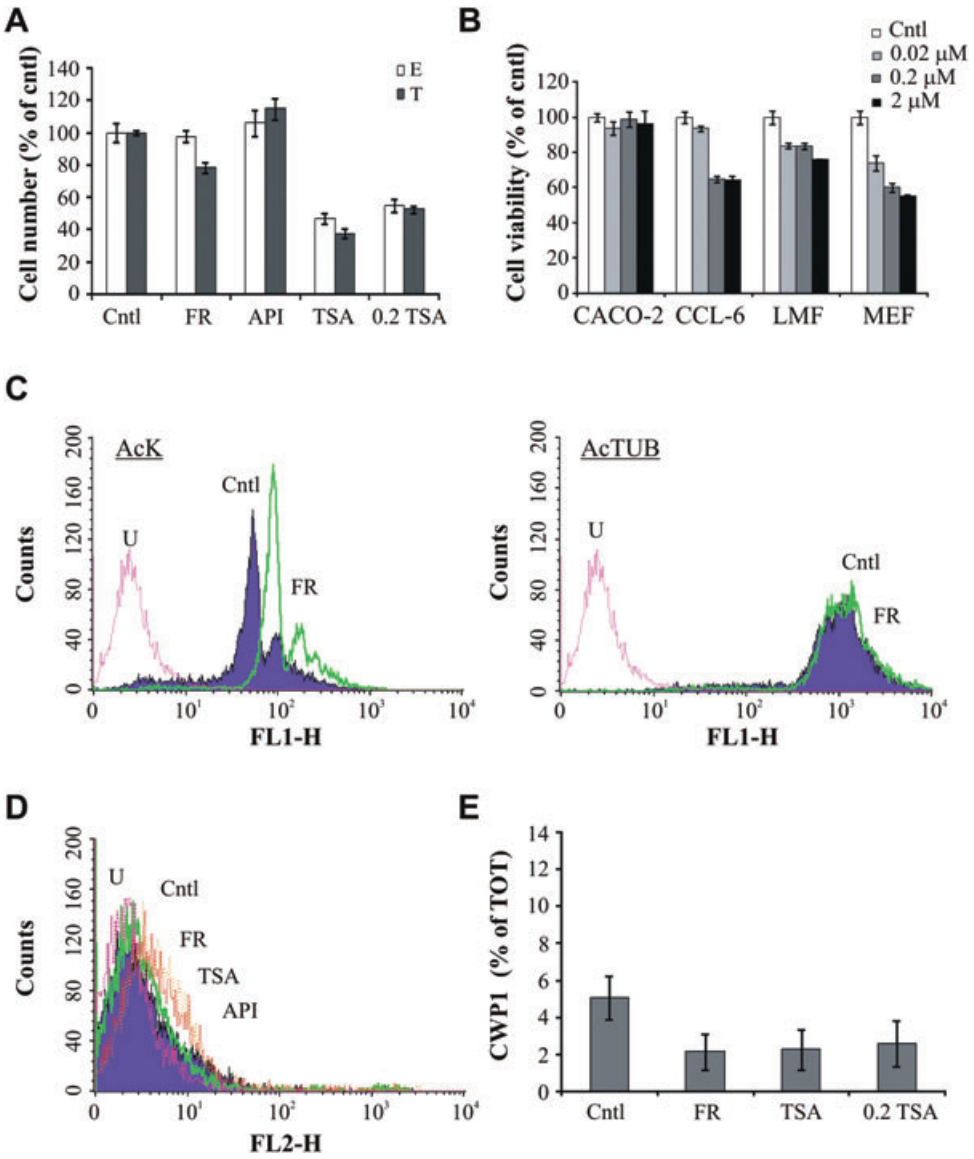

Fig. 7. FR235222 treatment of trophozoites does not induce parasite encystation.
A. Trophozoites (T) and encysting parasites (E) were treated for 24 h with 2 µM of the HDAC inhibitors FR235222 (FR), apicidin (API), Trichostatin A (TSA), 0.2 µM TSA or solvent (Cntl). Parasite numbers are expressed as percentage of untreated samples (Cntl). Data are average ± standard errors ($n = 9$) of a representative experiment done in duplicate.
B. Viability of mammalian cells treated for 24 h with solvent (Cntl) or FR235222 at the indicated concentrations was assessed by measuring AlamarBlue reduction (Biosource). Results of a representative experiment are presented as percentage of control ± standard errors ($n = 3$).
C. Trophozoites were treated for 24 h with FR235222 and levels of AcK (left panel) and acetylated tubulin (right panel) were quantified by flow cytometry. Overlay histograms showing cells unstained (U), treated with solvent (Cntl) or 2 µM FR235222 (FR).
D. Trophozoites were treated for 24 h with 2 µM FR235222 (FR), apicidin (API), Trichostatin A (TSA), or solvent (Cntl) and probed for CWP1. Overlay histogram of the treated cells is shown. U, unstained cells. Note the absence of CWP1 induction upon drug treatment.
E. Cells were treated for 24 h with 2 µM FR235222 (FR), Trichostatin A (TSA), 0.2 µM TSA or solvent (Cntl) and analysed by immunofluorescence. Number of parasites expressing CWP1 was expressed as percentage of the total number of parasites, assessed by nuclear staining, ±standard errors ($n = 6$).

differentiation, we quantified the expression of the encystation-induced protein CWP1 in presence of the HDACi FR235222, TSA or apicidin. Flow cytometry analysis (Fig. 7D) and enumeration of CWP1-expressing parasites by manual counting (Fig. 7E and Fig. S4) did not reveal any increase in CWP1 expression in presence of the inhibitors tested compared with control cells. In addition, no giardial 14-3-3 re-localization to the parasite nuclei was detected in the presence of FR235222 (Fig. S5), as is typically observed during parasite encystation (Lalle *et al.*, 2006). Collectively, these data indicate that treatment of trophozoites with HDACi did not

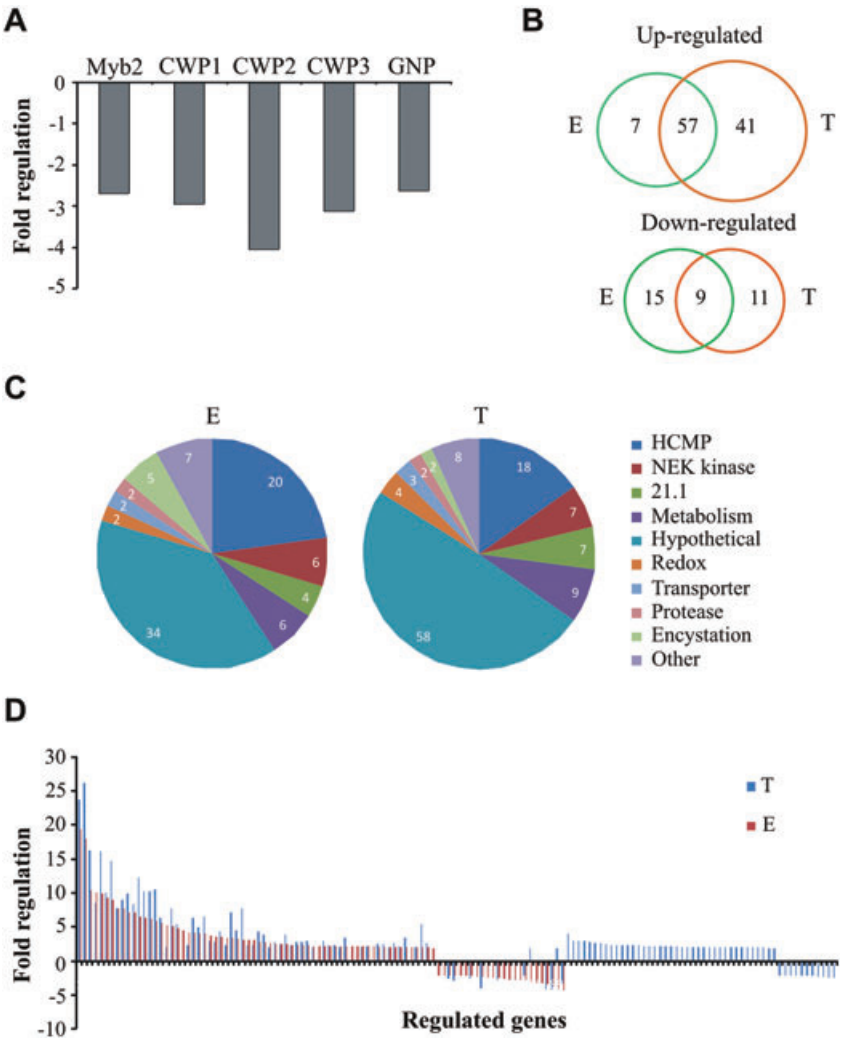

Fig. 8. FR235222 treatment modulates gene expression. RNA extracted from encysting cells and trophozoites treated for 15 h with 2 μM FR235222 or solvent were used for dual channel microarray analysis. The comparison of the transcription profiles of treated versus untreated samples are shown.
A. Drug treatment of encysting cells downregulated the expression of known encystation-specific genes. Names and *Giardia* DB accession numbers are the following: Myb1-like protein, Myb2 (GL50803-8722); cyst wall protein 1, CWP1 (GL50803-5638); cyst wall protein 2, CWP2 (GL50803-5435); cyst wall protein 3, CWP3 (GL50803-2421); glucosamine-6-phosphate deaminase, GNP (GL50803-8245).
B. Venn diagram of genes regulated by FR235222 in encysting cells (E) and trophozoites (T). No prominent overlap of genes regulated by FR235222 was observed in the opposite direction: only two genes downregulated in encysting cells were upregulated in trophozoites and none of the genes upregulated in encysting cells was downregulated in trophozoites.
C. Functional classes defined by Gene Ontology (GO) terms of the FR235222 regulated genes in encysting cells (E) and trophozoites (T).
D. Pattern of gene upregulated and downregulated following FR235222 treatment of encysting cells (E) and trophozoites (T).

promote but rather decreased the rate of spontaneous encystation.

FR235222 alters gene expression in encysting cells and trophozoites

As changes in histone acetylation are known to modulate gene transcription, we used a genome-wide approach to investigate whether FR235222 treatment modified the expression of a specific range of genes or induced a general modulation of the expression profile in *G. lamblia*. Transcriptomes of both encysting cells and trophozoites cultured in presence or absence of the inhibitor were compared by microarray analysis. cDNA was labelled with either Cy5-dUTP (FR235222-treated) or Cy3-dUTP (control), hybridized to a *G. lamblia* microarray, and genes whose expression varied by a minimum of twofold following inhibitor treatment were considered significantly regulated ($P < 0.01$).

Overall, 88 genes in encysting cells and 118 genes in trophozoites were found to be differentially regulated by FR235222 (Fig. S6), corresponding to ~2% of the 4969 currently predicted *Giardia* genes, and to ~1% of the total 9747 genes, including putative deprecated ones. The majority of the genes were upregulated in both the parasite stages, indicating that HDAC inhibition acted primarily by promoting gene transcription of a selected set of genes. However, in encysting cells treated with FR235222, induction of five genes crucial for parasite encystation was blocked, namely the DNA-binding transcription factor Myb2 (Sun *et al*., 2002; Huang *et al*., 2008), the three structural proteins forming the protective cyst wall (CWPs 1–3) and glucosamine-6-phosphate deaminase (GNP, also known as G6PI-B), which is involved in the biosynthesis of the cyst wall polysaccharide (Knodler *et al*., 1999) (Fig. 8A). These data also confirms that the lack of CWP1 induction in encysting parasites treated with FR235222 is due to reduced mRNA levels.

FR235222 upregulates the expression of identical genes in the two life stages of the parasite

We then compared the transcriptomes of encysting cells and trophozoites to test whether the transcriptional response to inhibitor treatment was similar in the two stages of the *G. lamblia* life cycle. Using Gene Ontology predictions of the *Giardia* Genome database, we grouped the FR235222-regulated genes into functional classes. Figure 8C shows the striking similarity of the gene classes modulated in encysting cells and trophozoites. The family of high cysteine membrane proteins (Davids *et al.*, 2006) was a highly represented class, which also showed the highest level of upregulation. Other highly represented classes were kinases of the NEK family, proteins annotated as 21.1 and proteins involved in metabolic functions. While many of the regulated genes had gene annotations in the *Giardia* Genome database, a considerable number of the genes indentified in both experimental conditions (38% in encysting cells and 49% in trophozoites) were hypothetical proteins of unknown function.

The set of genes modulated by FR235222 not only belonged to similar gene classes but also overlapped considerably in the two experimental conditions (Fig. 8B and D). Of the 64 genes upregulated in encysting cells, 57 were also found to be upregulated in trophozoites, while of the 24 downregulated genes, 9 were in common with the trophozoite gene list. No correlation was found in the opposite direction: in encysting cells only two of the downregulated genes were upregulated in trophozoites, and none of the upregulated gene was downregulated in trophozoites. Interestingly, all of the high cysteine membrane proteins identified in our array were upregulated in both encysting cells and trophozoites (with one exception in the trophozoites). Similarly, all the NEK kinases and all but one of the 21.1 proteins were upregulated in both parasite stages.

In order to determine whether the genomic environment plays a role in the expression of FR235222-regulated genes, we asked whether regulated genes were clustered. All regulated genes were distributed on 17 genomic scaffolds and a positive correlation was found between the number of regulated genes and the number of genes present on a given scaffold (Fig. S7A). Analysis of the gene position in the genomic scaffolds revealed that the regulated genes were not distributed in tight clusters containing multiple consecutive genes (Fig. S7B); in addition, regulated genes belonging to the same gene classes were not located in the same genomic location, indicating that physical proximity is not required for FR235222-induced transcriptional co-regulation. However, statistical approaches based on graphical and numerical computations revealed small groups of potentially co-regulated genes, which were distributed non-randomly in scaffolds CH991762 and CH991763 in encysting cells, and in scaffold CH991763 in trophozoites (Figs S7C and S8). The biological significance of these findings remains to be determined.

Validation of gene expression regulation

To confirm the expression patterns observed by microarray analysis, we performed RT-PCR of selected genes using RNA extracted from FR235222-treated trophozoites and encysting cells. Specifically, in the trophozoite sample we analysed two genes whose expression was upregulated upon FR235222 treatment (GL50803-114930 and GL50803-112153), while in the encysting cell sample we assessed the abundance of CWP1 transcript, whose expression was downregulated upon inhibitor treatment. Analyses of genes which were not regulated by the inhibitor (GL50803-117204 and GL50803-9558) or not transcribed (tubulin promoter sequence; Elmendorf *et al.*, 2001) were used as a loading and as a negative control respectively. In each case, the abundance of transcripts detected by RT-PCR confirmed the microarray data (Fig. 9A). Importantly, PCR reactions using the original, non-retro-transcribed RNA as template did not give any detectable products, confirming the absence of contamination with genomic DNA (not shown).

In addition, FR235222-induced upregulation of gene expression was further confirmed at the protein level. An N-terminal HA epitope tagged variant of the gene product, GL50803-17120, whose expression increased in both encysting cells and trophozoites upon inhibitor treatment, was expressed in trophozoites. As seen in the RT-PCR results, immunofluorescence and flow cytometry analyses substantiated the increased expression in presence of the inhibitor (Fig. 9B). Collectively, these results unambiguously validate the microarray data both at the transcriptional and translational level.

Discussion

Giardia lamblia encystation is critical for both parasite survival outside the host and disease transmission. Despite the considerable amount of information available on *G. lamblia* encystation at the cellular level, the molecular underpinnings of its regulation remain limited. In the present study, we investigated the role of epigenetic chromatin modification in the parasite stage differentiation. We found that exposure of parasites to the HDACi FR235222 increased the levels of histone acetylation, altered gene transcription and inhibited *G. lamblia* encystation, thus providing the first evidence that epigenetic mechanisms control stage differentiation in this parasite. Notably, FR235222 treatment effectively inhibited CWP1 expression at low nanomolar concentrations, suggesting that the

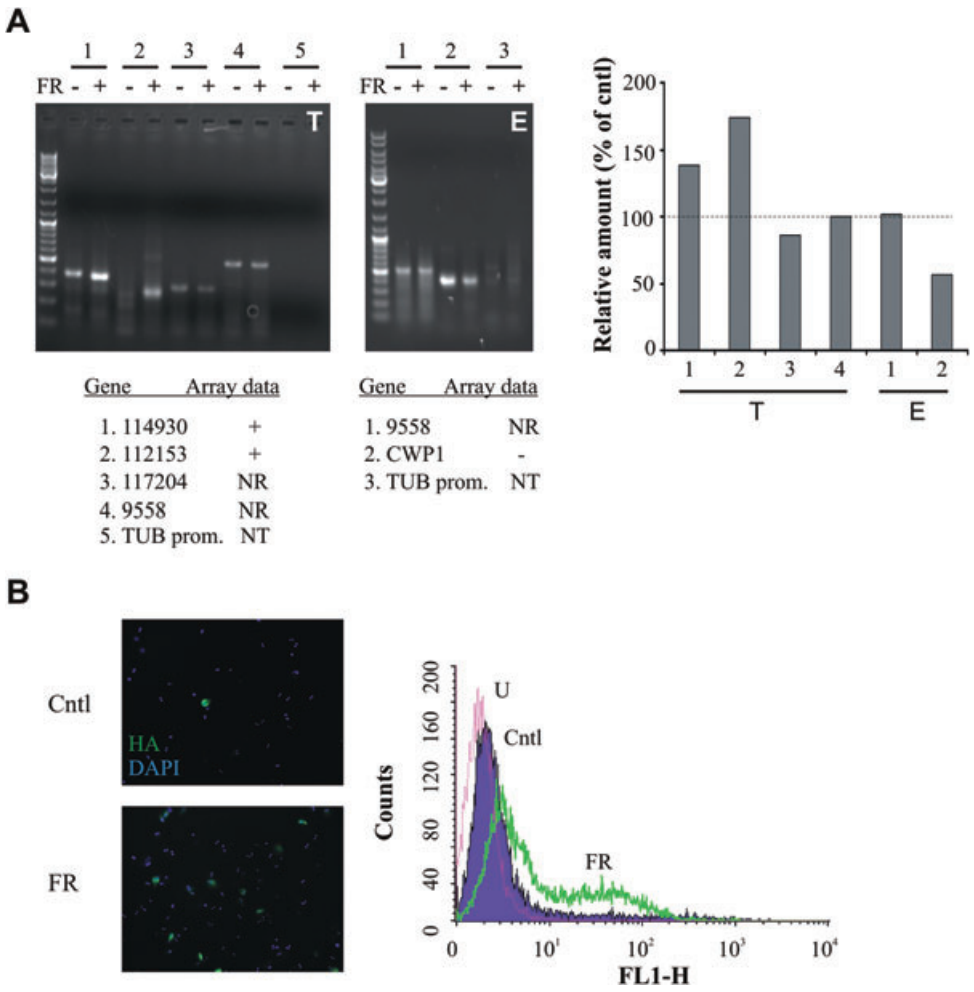

Fig. 9. Confirmation of microarray data.
A. RNA extracted from trophozoites and encysting cells treated for 15 h with 2 μM FR235222 or solvent were tested by reverse transcriptase (RT)-PCR for the transcription of regulated and not regulated gene products. Primer pairs binding to the tubulin (TUB) promoter were used as negative control. The obtained amplification products confirmed the gene regulation observed by microarray analysis. +, upregulated; –, downregulated; NR, not regulated; NT, not transcribed. Right panel, densitometric quantification of the relative amount of the gene products upon FR235222 treatment expressed as percentage of untreated control (Cntl).
B. The gene product GL50803-17120, whose expression was upregulated by 2 μM FR235222 in both encysting cells and trophozoites, was HA-tagged and episomaly expressed under control of its endogenous promoter. Encysting parasites were treated with 2 μM FR235222 (FR) or solvent (Cntl) and the expression of the recombinant protein monitored by immunofluorescence (left panel) and flow cytometry (right panel) analyses. Note the increased expression of the protein upon drug treatment. DAPI, nuclear staining. U, unstained cells.

observed phenotype is a consequence of specific inhibition of giardial HDAC. In addition, the fact that only 1–2% of predicted genes are affected and that clear functional categories are identified argues against a random off-target effect.

A highly reduced histone deacetylation machinery is present in G. lamblia

Giardia lamblia has a compact genome organization and few identified regulatory elements, consistent with significant reductive evolution (Morrison *et al.*, 2007). Thus, this protist is considered an interesting model for investigating minimized cellular systems. Analysis of the parasite genome revealed the occurrence of genes coding for putative chromatin modifying proteins, including HATs, deacetylases and methylases, suggesting that mechanisms for epigenetic regulation of gene expression are present in this parasite. Interestingly, demethylases seem to be absent in *G. lamblia*, *Trichomonas*, *Entameba histolytica* and microsporidians, indicating that demetylase activity is dispensable for these parasites or carried out by unrelated enzymes (Iyer *et al.*, 2008).

Consistent with its reduced cellular machinery, only one classical HDAC homologue is annotated in the *G. lamblia* genome (GL50803-3281) and its nuclear localization

further supports a deacetylase activity on histone proteins. The presence of a single HDAC is in striking contrast with the size of the HDAC repertoire found not only in metazoan but also in unicellular protozoa, including the apicomplexan *T. gondii* with five putative HDACs. It is worth mentioning that a single representative of class I HDACs was identified so far in another enteric parasite, *Entamoeba hystolitica*, suggesting that simplified mechanisms for regulating histone acetylation are operational in basal organisms (Ramakrishnan *et al.*, 2004).

Sequence alignments, 3D modelling and prediction of inhibitor binding mode highlighted the high degree of giardial HDAC conservation, in particular at the catalytic site. Moreover, compared with the five *T. gondii* HDACs, giardial HDAC showed the highest degree of similarity with HDAC3, the target of FR235222, further arguing for a specific interaction of the inhibitor with the giardial enzyme.

Of note, the sequence of giardial HDAC contains a four-amino-acid insertion (position 283–286) not found in other species. While amino acid insertions appear to be common in *G. lamblia* proteins, as exemplified by giardial histone acetyl transferase (Morrison *et al.*, 2007), their size is typically larger (20 amino acids on average). The significance of the extra amino acids in the giardial HDAC is unknown.

Histone acetylation regulates stage-specific gene expression during G. lamblia *encystation*

We obtained three lines of evidence indicating that epigenetic mechanisms are involved in regulating expression of encystation-specific genes. First, we observed that the level of histone acetylation decreased during encystation, which is consistent with the parasites differentiating to a dormant stage. Based on this, we can formulate the hypothesis that the high acetylation levels effectively make the parasite refractory to entering differentiation after going through the S-G2 transition of the cell cycle (Bernander *et al.*, 2001). Second, we tested this hypothesis by actively increasing the acetylation levels during encystation. This reduced the synthesis of a relatively small subset of gene products and specifically blocked induction of all known encystation-specific genes. This reveals an as yet unknown level of stage-specific control of encystation-specific genes in addition to the regulation by transcription factors. Importantly, we showed that short-flanking regions of encystation-specific proteins are sufficient for the FR235222-mediated inhibition of gene expression, indicating that no distant regulatory elements are required for modulation of these genes. Third, we demonstrated that histone hyperacetylation altered gene transcription; while the majority of FR235222-responsive genes were upregulated, the mRNA of encystation-specific genes were downregulated. Taken together, our data indicate that chromatin acetylation states play a key role in the regulation of parasite differentiation by controlling the level of gene transcription, possibly by altering the accessibility of the promoter region to Myb2 and other *cis*-acting factors implicated in regulation of encystation-specific genes.

Although we unambiguously showed that increased histone acetylation repressed the transcription of encystation-specific genes, this repression challenges the classical view where histone hyperacetylation is associated with increased gene transcription. Interestingly, inhibition of stage differentiation in response to selected HDACi, TSA and HC-toxin, but not apicidin, has also been reported in *Entamoeba* parasites, but the molecular mechanism still remains to be investigated (Byers *et al.*, 2005).

One plausible explanation is that the repression of encystation-specific gene expression in *G. lamblia* is indirect and occurs via the action of a repressor, which is in turn positively regulated by the increased histone acetylation. The identification of negative *cis*-active elements in the CWP2 promoter (Davis-Hayman *et al.*, 2003) further supports the presence of a repressor mechanism to maintain low levels of encystation-specific proteins during vegetative growth. Block of upregulation of the *trans*-activator transcription factor Myb2 in presence of FR235222 suggests that the putative repressor may act upstream of Myb2 activation.

In other protozoa such as *Toxoplasma gondii* and *Entamoeba histolytica* it has been proposed that HDAC regulation of specific genetic loci is stage-specific, and HDAC inhibition during encystation may derepress trophozoite-specific genes in *E. histolytica*, thus arresting parasite differentiation (Saksouk *et al.*, 2005; Ehrenkaufer *et al.*, 2007). However, our findings suggest in several ways that *G. lamblia* may possess a simpler HDAC regulation, namely (i) only one classical HDAC is found in the parasite genome, arguing against the presence of stage-specific differential HDAC expression; (ii) using the HDACi FR235222, we found increased acetylation in both trophozoites and encysting cells, suggesting that giardial HDAC is indeed operational in both parasite stages; and (iii) contrary to what was observed in *T. gondii* and *E. histolytica* (Ehrenkaufer *et al.*, 2007; Bougdour *et al.*, 2009), HDACi treatment of trophozoites does not trigger parasite stage conversion, suggesting that a trophozoite-specific HDAC engaged in the repression of encystation-specific genes is not present in *G. lamblia*. On the other hand, we showed that the levels of histone acetylation decreased in encysting cells compared with trophozoites. While we cannot exclude that this decrease is due to a reduced activity of histone

acetyltransferases, inhibition of HDAC was sufficient to reverse the phenomenon and to block encystation. Hence it is likely that *G. lamblia* does not rely on several stage-specific HDACs but rather on a single HDAC, whose activity is differentially modulated in the parasite life stages, possibly by binding with different stage-specific partners via its C-terminal domain (Pflum *et al*., 2001). In this context, the regulation of HATs and deacetylases in the different stages of *G. lamblia* is worthy of careful characterization.

Finally, in light of ever-increasing indications that HDACs also function as activators of transcription in yeast (Kurdistani and Grunstein, 2003), we cannot dismiss the possibility that the FR235222-mediated inhibition of encystation-specific gene expression may be a direct consequence of the blocked HDAC activity. Future analyses to determine the acetylation pattern of encystation-specific genes will help to further our understanding of the epigenetic regulation mechanisms that control stage differentiation in this parasite.

Whole-genome transcriptome regulation upon HDAC inhibition

Our microarray data revealed that FR235222 treatment changed gene expression in both encysting cells and trophozoites. The observed gene regulation is likely to result from a selective inhibition of giardial HDAC and not due to drug-induced lethality, as treated parasites were able to replicate normally in presence of the inhibitor. In addition, analysis of microarray evidence available in the *Giardia* Genome Database revealed that all but three genes regulated by FR235222 treatment were not regulated during stress induction (not shown), indicating that the changes of mRNA levels induced by FR235222 do not result from an inhibitor-induced stress response. Finally, the percentage of genes whose expression was changed by FR235222 was quite small (~2%) and of a similar range to what reported for the treatment with the HDACi TCA in mammalian cells (Heller *et al*., 2008) and *E. histolytica* (Ehrenkaufer *et al*., 2007).

Analysis of the modulated genes revealed that, in marked contrast with other cyst-forming parasites *T. gondii* and *E. histolytica*, treatment of *G. lamblia* trophozoites with HDACi did not induce the expression of encystation-specific genes, suggesting that repression of such genes during the vegetative trophozoite stage is not likely to be maintained solely by HDAC activity.

Further comparison of gene expression in encysting cells and trophozoites showed that the genes sensitive to FR235222 were strikingly similar in the two stages of the parasite life cycle. This overlap in expression profile emphasizes that the developmental program is accomplished with only very few changes in the global expression pattern. Besides hypothetical proteins, the major class of upregulated genes was high cysteine membrane proteins (HCMp), a recently described family (Davids *et al*., 2006) whose function in *G. lamblia* remains enigmatic. While we found that the expression of 26% of the known HCMp genes is modulated by FR235222, only ~1% of the previously mentioned VSP family, also composed of cysteine rich proteins, was affected. The result was quite surprising, as histone acetylation of the upstream region of VSP was proposed to positively regulate the expression of the single VSP variant present on the cell surface at any given time, and thus acting as a master regulator of antigenic variation in *G. lamblia* (Kulakova *et al*., 2006). The fact that inducing histone hyperacetylation did not result in a general increase in VSP expression suggests that the epigenetic histone modification by the acetylation mark may not be sufficient to promote VSP transcription, and that additional mechanisms are required to regulate the expression of these proteins. Alternatively, the use of different *G. lamblia* isolates (WB, prototype of Assemblage A in our study, and GS, prototype of Assemblage B in Kulakova *et al*., 2006) might also account for some differences in gene regulation, as the two isolates present different phenotypes *in vitro* and *in vivo* (Franzen *et al*., 2009; Monis *et al*., 2009).

The other two protein families whose expression was modulated by FR235222 were cytoskeletal proteins 21.1 and members of the NIMA-related protein kinases (NEK) (Morrison *et al*., 2007). The latter are widely represented in eukaryotes, but their role remains poorly characterized. Interestingly, the NEK family shows a significant expansion in *G. lamblia*, where it constitutes the majority of the parasite kinome (Morrison *et al*., 2007). The significance of this expansion is currently unknown.

Finally, genes of the proteins and protein families significantly affected by FR235222 treatment were scattered in different scaffolds of the parasite genome, indicating that HDAC inhibition can modulate the expression of functionally related genes independent of their genomic location. It is worth noting that statistical approaches identified three examples of non-randomly distributed gene sets in both encysting cell and trophozoite transcriptomes. Interestingly, the cluster found in trophozoites contained the CWP1 gene surrounded by four upregulated genes. As CWP1 mRNA was found to be slightly upregulated in our trophozoite array without detecting parasite stage differentiation, it is possible that the CWP1 genomic surrounding may have influenced CWP1 transcription without activation of the complete encystation program.

In conclusion, we showed, for the first time, that HDAC inhibition increased histone acetylation and induced transcriptional changes in *G. lamblia*, substantiating the presence of an evolutionarily conserved mechanism for epigenetic regulation of gene expression in this early

divergent parasite. In addition, we provided evidence that the HDAC repertoire is highly reduced and the phenotypic and transcriptional responses following HDAC inhibition are simpler in *G. lamblia* than in other cyst-forming parasites, indicative of the minimized cellular processes typical of this parasite. Lastly, we discovered that HDAC inhibition, while not affecting parasite replication, potently blocked *G. lamblia* encystation and that short-flanking regions of encystation-specific proteins were sufficient for the drug-mediated repression of gene expression. Collectively, these results reveal that the transcriptional changes during stage differentiation are under the control of epigenetic regulation, and further illuminate the poorly understood mechanisms of gene regulation in this parasite. Additionally, our findings clearly demonstrate that HDAC activity is a promising target for pharmacological agents aiming to effectively block the production of *G. lamblia* cysts and thus reduce disease transmission.

Experimental procedures

Biochemical reagents

Unless otherwise stated, all chemicals were purchased from Sigma and cell culture reagents from Gibco-BRL. Inhibitor stock solutions were prepared at the following concentrations: 179 mM FR235222, 1.6 mM apicidin, 1 mM TSA, 2.29 mM HC-toxin, 3.06 mM scripaid. Inhibitors were freshly diluted to the concentrations required for the individual experiment.

Parasite and tissue culture

Trophozoites of the *Giardia lamblia* strain WBC6 (ATCC catalog number 50803) were grown axenically as described (Sonda *et al*., 2008). Harvested parasites were counted using the improved Neubauer chamber. New subcultures were obtained by inoculating 5×10^4 trophozoites from confluent cultures into new 11 ml culture tubes. Two-step encystation was induced as described previously (Gillin *et al*., 1989) by cultivating the cells for ~44 h in medium without bile (pre-encysting medium) and subsequently in medium with higher pH and porcine bile (encysting medium).

Drug treatment of trophozoites was performed by incubating sub-confluent cultures for 24 h with the inhibitors at the concentrations indicated in the figure legend of the individual experiments. Drug treatment of encysting cells was performed in two steps: 8 h drug incubation in pre-encysting medium and additional 16 h incubation in encysting medium. Viability of cysts following drug treatment was tested by trypan blue exclusion (Aley *et al*., 1994).

Mammalian cells used in this study were: Caco-2 (human colon adenocarcinoma, ATCC HTB 37), Intestine 407 (human embryonic jejunoileum, ATCC CCL-6), primary lung fibroblasts isolated from 6- to 8-week-old mice kindly provided by E. Gulbins (University of Duisburg-Essen, Essen, Germany) and mouse embryonic fibroblasts kindly provided by A. Schinkel (the Netherlands Cancer Institute, Amsterdam, The Nederlands). Cells were routinely cultured in Dulbecco's modified Eagle's medium or minimum essential media supplemented with non-essential amino acids and sodium pyruvate, in case of primary fibroblasts. All media were supplemented with 10% fetal calf serum, 2 mM glutamine, 50 U of penicillin ml^{-1}, and 50 μg of streptomycin ml^{-1}. Cultures were maintained at 37°C with 5% CO_2 in tissue culture flasks and trypsinized at least once a week.

Expression vector construction and transfection

The plasmid for episomal expression of haemagglutinin (HA)-tagged GlHDAC (GL50803-3281) under control of CWP1 promoter was based on the expression cassette C1-CWP (Hehl *et al*., 2000). The plasmid for stable expression of HA-tagged Sar1 under control of CWP1 promoter was engineered as described (Stefanic *et al*., 2009). The plasmid for the episomal expression of HA-tagged GL50803-17120 was based on the expression cassette C1-CWP where the CWP1 promoter was replaced by the endogenous promoter. Oligonucleotides (5′–3′ orientation) used for the construct were the following: for GL50803-3281, PstI-s CGCTGCAGATGCCGC CTTCAAAACCCTC and HA-PacI-as CGTTAATTAACTACG CGTAGTCTGGGACATCGTATGGGTAGTTCTCATCTAACC CCGCTTC; for GL50803-17120, XbaI-s CGTCTAGACTAC TATGGATGAAGCCGAG and HA-NsiI-as CGATGCATC GCGTAGTCTGGGACATCGTATGGGTAAATCGTGATGTTG TTAGTTAAAC, encoding the HA epitope tag for the amplification of 200 bp upstream the starting codon containing the endogenous promoter followed by the protein leader sequence; 17120-NsiI-s CGATGCATGGTGTCCGCGAAG GAAAATATG and 17120-PacI-as CGTTAATTAACTAGC TATAAATGGCTGCAATG for the amplification of the GL50803-17120 coding sequence.

15 μg of plasmid vector DNA was electroporated (350 V, 960 μF, 800 Ω) into trophozoites. For stable genome integration, the plasmid DNA was linearized using SwaI restriction enzyme before electroporation. Linearized plasmid targets the *G. lamblia* triose phosphate isomerase locus (GL50803-93938) and integration occurs by homologous recombination under selective pressure with the antibiotic puromycin (Jimenez-garcia *et al*., 2008).

Gene expression analysis

Trophozoites were treated for 15 h with 2 μM FR235222 or solvent; encysting cells were similarly treated in two steps: 8 h drug incubation in pre-encysting medium and additional 7 h incubation in encysting medium. RNA was isolated using an RNAeasy kit (Qiagen, Stanford, CA) following the 'Animal Cells Spin' protocol. Residual genomic DNA was removed with DNase 1 digestion according to the manufacturer's protocol. The integrity of the RNA was analysed in a Bioanalyser (Agilent Technologies, Palo Alto, CA, USA) with 'Eukaryote Total RNA Nano Series II' settings.

For dual channel microarray analysis, extracted total RNA was processed using the Amino Allyl MessageAmpII a RNA Amplification Kit (Ambion, Austin, TX, USA) and labelled with *N*-hydroxysuccinimidyl ester-derivatized reactive dyes Cy3 or Cy5, according to the manufacturer's protocol. After purifica-

tion, 2 μg each of Cy3 or Cy5 labelled aRNA was denatured, added to SlideHyb Buffer I (Ambion), and hybridized to *G. lamblia* microarrays version 2 (TIGR) in a Tecan HybStation at the Functional Genomics Centre Zurich, Switzerland. The arrays are aminosilane surface coated glass slides with 9115 oligonucleotides (70mers) designed to cover the whole *G. lamblia* WBC6 strain genome.

Prior to hybridization, slides were hydrated and blocked with 150 μl BSA buffer (0.1 mg ml^{-1} BSA, 0.1%SDS in 3× SSC buffer) for 1 h at 42°C. After washing, samples were injected and hybridized for 16 h at 42°C. Slides were scanned in an Agilent Scanner G2565AA, using laser lines 543 nm and 633 nm for excitation of Cy3 and Cy5 respectively. Spatial scanning resolution was 10 μm, single pass. The scanner output files were quantified using the Genespotter Software (MicroDiscovery GmbH, Berlin, Germany) with default settings and 2.5 μm radius. The median spot intensities were evaluated with the Web application MAGMA (Rehrauer *et al*., 2007) and normalized using the print-tip-wise loess correction of the *limma* package (Smith, 2005). Potential gene-specific dye-effects were estimated from self–self hybridizations. Differential expression of genes during FR235222 treatment is reported as the log_2 of the drug-induced fold-change compared with control treated samples, as well as the *P*-value for differential expression as estimated by the empirical Bayes model implemented in *limma*. All reactions were performed in triplicate.

Semi-quantitative reverse transcriptase polymerase chain reaction

300 ng of the isolated RNA described above was mixed with 10 μM k-anchorV primer and cDNA was synthesized using the Quiagen Omniscript Kit (Qiagen, Stanford, CA, USA) according to the manufacturer's protocol. Fifty-fold dilutions of cDNA were used as template for PCR amplification using 0.4 μM each of gene-specific forward primers and a k-adaptor reverse primer. PCR products were separated on 1.5% agarose gels, visualized with ethidium bromide, and images recorded in a MultiImage Light Cabinet with AlphaEaseFC software (Alpha Innotech, San Leonardo, CA, USA). Primers used in the study are: k-anchorV, CCGGAATT CGGTACCTCTAGA(T18)V; k-adaptor, CCGGAATTCGGTAC CTCTAGA; Tubulin, ATTTAGAATTCAAATCAGCAAATTC; 114930, GCCAGGGCCTCATCGAAC; 117204, ATACGTGG GGGTGGAGAAC; 112135, CGTCCTCTGCTACTCCTTTG; 9558, CGGACCATTACTTCTACGTACT; CWP1, CTGGTA CATGAGTGACAACGCT.

Fluorescence microscopy and flow cytometry analysis

For immunolabelling, harvested cells were washed twice in ice-cold PBS, and fixed with 3% formaldehyde solution in PBS. Fixed cells were blocked, with or without previous permeabilization with 0.2% Triton X-100 in PBS for 20 min, and incubated with primary antibodies for 1 h. The primary antibodies used in this study were: anti-acetyl lysine rabbit antiserum (Abcam, Cambridge, MA, USA), 1:500 dilution; anti-acetylated tubulin (Sigma), 1:500 dilution; Cy3-conjugated anti-CWP1 mouse monoclonal antibody (Waterborne, New Orleans, LA, USA), 1:60 dilution; anti-clathrin heavy chain mouse antiserum (Marti *et al*., 2003), 1:2000 dilution; anti-protein disulphide isomerase 2 (PDI2) mouse antiserum, 1:1000 dilution; anti-Sar1 mouse antiserum (Stefanic *et al*., 2009), 1:300 dilution; Alexa488-conjugated anti-HA mouse monoclonal antibody (Roche Diagnostics GmbH, Manheim, Germany) 1:30 dilution; anti-giardial 14-3-3 (Lalle *et al*., 2006) 1:50 dilution, kindly provided by M. Lalle (Istituto Superiore di Sanita', Rome, Italy). Fluorophore-conjugated secondary antibodies were purchased from Invitrogen (Basel, Switzerland) and used at 1:200 dilution. Microscopy analyses were performed on a Leica DM IRBE fluorescence microscope (Leica Microsystems, Wetzlar, Germany) using the appropriate settings. Single-cell quantification of fluorescence was performed using a FACSCalibur flow cytometer (Becton & Dickinson, Basel, Switzerland).

Mammalian cells metabolic assay

The metabolic activity of mammalian cells was tested by using the AlamarBlue assay (Biosource, Camarillo, CA, USA). Briefly, mammalian cells were grown to confluence or semi-confluence in 96-well plates, incubated for 24 h with FR235222 at the concentrations indicated in the figure legend, and processed according to the manufacturer's instructions. For co-culture experiments, cells were seeded in 96-well plates at 3×10^4 cells per well and incubated for 24 h to confluence. Harvested *G. lamblia* trophozoites were added to the cell monolayers at 6×10^4 parasites per well, followed by 24 h incubation with 2 μM FR235222 and viability assay.

Western blot analysis of nuclear proteins

Encysting cells were treated with 2 μM FR235222 as described before. Nuclear extracts were prepared by mild detergent lysis as described (Bougdour *et al*., 2009). Briefly, 6×10^7 cells were collected, washed in ice-cold PBS and resuspended in 700 μl lysis buffer [10 mM HEPES, 10 mM KCl, 1.5 mM $MgCl_2$, 0.5 mM dithiothreitol (DTT), 0.5% NP-40, 1 mM PMSF and protease inhibitor cocktail]. The nuclear pellet was collected by centrifugation at 10 000 *g* for 10 min at 4°C and acid extracted for 2 h by adding 200 μl each of 5 M $MgCl_2$ and 0.8 M HCl. Insoluble material was removed by centrifuging at 13 000 *g* for 10 min at 4°C and soluble proteins containing basic histones were precipitated with 25% TCA. Precipitated proteins were washed twice with ice-cold acetone and resuspended in 100 μl H_2O. Aliquots corresponding to 16 μg of proteins were analysed by SDS-PAGE on a 15% gel followed by Coomassie blue staining and probed, following Western blotting, using the previously described anti-acetyl lysine rabbit antiserum (Abcam) at 1:2000 dilution. Immunoreactive bands were visualized with horseradish peroxidase-conjugated secondary antibodies and enhanced chemiluminescence.

Determination of protein concentration

Protein content was determined using the Bio-Rad Protein Assay according to the instructions provided by the manufacturer. Bovine serum albumin was used for the standard curve.

Mass spectrometry identification of histones

Trophozoites were treated with 2 μM FR235222 for 24 h, harvested and washed in ice-cold PBS. 3×10^7 cells were then resuspended in 500 μl lysis buffer (10 mM HEPES, 10 mM KCl, 1.5 mM $MgCl_2$, 0.5 mM DTT, 0.5% NP-40, 1 mM PMSF and protease inhibitor cocktail), incubated for 30 min at 4°C, and the nuclear pellet was collected by centrifugation at 10 000 *g* for 10 min at 4°C. The pellet was resuspended in 5 ml IP buffer (10 mM HEPES, 10% glycerol, 5 mM EDTA, 1% NP-40, 1 mM PMSF), sonicated and incubated with 5 μl anti-acetyl lysine rabbit antiserum overnight at 4°C, followed by addition of protein-A conjugated beads. After incubation at 4°C under rotary agitation for 5 h, the beads were washed, resuspended in 30 μl sample buffer, boiled and treated with 3.3 μl iodoacetamide (0.5 M in 1 M Tris-HCl pH 8.0) for 15 min at room temperature. Proteins were separated on a 15 % gel, stained using the mass spectrometry-compatible SilverQuest™ silver staining Kit (Invitrogen) and the excised bands analysed by peptide mass fingerprint using LC/MS/MS.

Protein structure prediction

The SWISS-MODEL web service (Guex and Peitsch, 1997; Schwede *et al*., 2003; Arnold *et al*., 2006) was used to build 3D models of GlHDAC and HsHDAC8. Docking of FR235222 in the catalytic site of GlHDAC was performed using the program WITNOTP (Armin Widmer, Novartis Pharma, Basel). Alignments were performed with Multalin (http://bioinfo.genotoul.fr/multalin/) and sequence comparisons were performed using Blast2.

Bioinformatic analyses

For visual identification of cluster candidates, we defined for each scaffold a metric M_f based on a potential function f analogous to the gravitational potential of mass points. In addition to a constant threshold, we used a linear combination $\mu_{pot} + \lambda s_{pot}^+$, based on mean μ_{pot} and conditional standard deviation s_{pot}^+ of all potential fields generated by all permutations of gene distributions. The metric M_f was used to calculate the cluster hierarchy on all levels by complete linkage. All clusters were ranked according to the calculated probability $p_{cluster}$, based on hypergeometric distributions. For the identification of statistically evident clusters, we defined approximate permutation tests based on the Null-hypothesis H_0 of random and uniform distribution of regulated genes within the scaffolds, and the three following test statistics: mean deviation X_1 and standard deviation X_2 of the number of not-regulated genes between two regulated genes, and maximum number of consecutive short intervals ($\leq k$) of non-regulated genes $X_{3,k}$ to account for the cluster size. The distributions of these test statistics were approximated by Monte Carlo sampling 100 000 random permutations for each scaffold. The functions used in this study were: $f(x)_{x \neq xi} := \Sigma_{(i=1,\ldots,n)} 1/(x - x_i)$, $f(x_i) := c << 0$; $M_f(x,y) := \max_{z \in [x,y]}(|f(x) - f(z)|)$; $f_{\boldsymbol{b}}(x)_{bx \neq 1} := \Sigma_{(i=1,\ldots,d)} b_i/(x - i)$, $f_{\boldsymbol{b}}(x)_{bx=1} := c << 0$; $\mu_{pot}(x) := (\Sigma_{\boldsymbol{p} \in \boldsymbol{P}} f_{\boldsymbol{p}}(x))/|\boldsymbol{P}|$; $(s_{pot}^+)^2 := (\Sigma_{\boldsymbol{Q} = \{\boldsymbol{p} | \boldsymbol{p} \in \boldsymbol{P} \wedge f_{\boldsymbol{p}}(x) > 0\}} (f_{\boldsymbol{p}}(x) - \mu_{pot}(x))^2)/|\boldsymbol{Q}|$; $p_{ClusterCa,b,r} := \Pr\{Y_{b\text{-}a\text{-}2,n,d} = r - 2\} \Pr\{Y_{2,2,n\text{-}(b\text{-}a\text{-}2)} = 2\}$, where d = number of genes of a scaffold, n = number of regulated genes in a scaffold, $x_1 < x_2 < \ldots < x_n$, $1 \leq x_i \leq d$ the positions (consecutive numbers) of the regulated genes, $\boldsymbol{b} = (b_1, b_2, \ldots, b_d)$, $b_i = \text{if}(i \neq x_i, 0, 1)$, $\boldsymbol{P}$ = set of all permutations of $\boldsymbol{b}$, $Y_{m,s,t}$ a hypergeometric random variable as m draws without replacement from a population of t genes, thereof s regulated, $C_{a,b,r}$ a cluster $\{a = x_1 < \ldots < b = x_i\}$ with r elements.

Acknowledgements

We thank Astellas Pharma for their kind gift of FR235222 compound, M. Lalle for kindly providing the anti-14-3-3 antibodies, Armin Widmer (Novartis Pharma, Basel) for the program WITNOTP, and Therese Michel for technical assistance.

Giardia lamblia microarrays (version 2) were kindly offered through NIAID's Pathogen Functional Genomics Resource Centre, managed and funded by Division of Microbiology and Infectious Diseases, NIAID, NIH, DHHS and operated by the J. Craig Venter Institute. The Functional Genomics Centre Zurich, Switzerland (http://www.fgcz.uzh.ch) is a joint facility of the ETH Zurich and the University of Zurich.

This work was supported by grants of the Marie Heim-Vögtlin Foundation and Fondation Pierre Mercier pour la Science to SS, of the Swiss National Science Foundation (Grant No. 3100A0-112327) to ABH, CNRS (ATIP+), Agence National de la Recherche (ANR-MIME program), and INSERM (Contrat d'Interface) to M.A.H.

References

Adam, R.D. (2001) Biology of *Giardia lamblia*. *Clin Microbiol Rev* **14:** 447–475.

Aley, S.B., Zimmerman, M., Hetsko, M., Selsted, M.E., and Gillin, F.D. (1994) Killing of *Giardia lamblia* by cryptdins and cationic neutrophil peptides. *Infect Immun* **62:** 5397–5403.

Arnold, K., Bordoli, L., Kopp, J., and Schwede, T. (2006) The SWISS-MODEL workspace: a web-based environment for protein structure homology modelling. *Bioinformatics* **22:** 195–201.

Bazan-Tejeda, M.L., Arguello-Garcia, R., Bermudez-Cruz, R.M., Robles-Flores, M., and Ortega-Pierres, G. (2007) Protein kinase C isoforms from *Giardia duodenalis*: identification and functional characterization of a beta-like molecule during encystment. *Arch Microbiol* **187:** 55–66.

Bernander, R., Palm, J.E., and Svard, S.G. (2001) Genome ploidy in different stages of the *Giardia lamblia* life cycle. *Cell Microbiol* **3:** 55–62.

Blagosklonny, M.V., Robey, R., Sackett, D.L., Du, L., Traganos, F., Darzynkiewicz, Z., *et al.* (2002) Histone deacetylase inhibitors all induce p21 but differentially cause tubulin acetylation, mitotic arrest, and cytotoxicity. *Mol Cancer Ther* **1:** 937–941.

Bolden, J.E., Peart, M.J., and Johnstone, R.W. (2006) Anticancer activities of histone deacetylase inhibitors. *Nat Rev Drug Discov* **5:** 769–784.

Bougdour, A., Maubon, D., Baldacci, P., Ortet, P., Bastien, O., Bouillon, A., *et al.* (2009) Drug inhibition of HDAC3 and epigenetic control of differentiation in Apicomplexa parasites. *J Exp Med* **206:** 953–966.

Byers, J., Faigle, W., and Eichinger, D. (2005) Colonic short-chain fatty acids inhibit encystation of Entamoeba invadens. *Cell Microbiol* **7:** 269–279.

Chen, Y.H., Su, L.H., Huang, Y.C., Wang, Y.T., Kao, Y.Y., and Sun, C.H. (2008) UPF1, a conserved nonsense-mediated mRNA decay factor, regulates cyst wall protein transcripts in *Giardia lamblia*. *PLoS ONE* **3:** e3609.

Clark, M., III, Cramer, R.D., and van Opdenbosch, N. (1989) Validation of the general purpose tripos 5.2 force field. *J Comput Chem* **10:** 982–1012.

Davids, B.J., Reiner, D.S., Birkeland, S.R., Preheim, S.P., Cipriano, M.J., McArthur, A.G., and Gillin, F.D. (2006) A new family of giardial cysteine-rich non-VSP protein genes and a novel cyst protein. *PLoS ONE* **1:** e44.

Davis-Hayman, S.R., Hayman, J.R., and Nash, T.E. (2003) Encystation-specific regulation of the cyst wall protein 2 gene in *Giardia lamblia* by multiple cis-acting elements. *Int J Parasitol* **33:** 1005–1012.

Dawson, S.C., Sagolla, M.S., and Cande, W.Z. (2007) The cenH3 histone variant defines centromeres in *Giardia* intestinalis. *Chromosoma* **116:** 175–184.

Dowling, D.P., Gantt, S.L., Gattis, S.G., Fierke, C.A., and Christianson, D.W. (2008) Structural studies of human histone deacetylase 8 and its site-specific variants complexed with substrate and inhibitors. *Biochemistry* **47:** 13554–13563.

Ehrenkaufer, G.M., Eichinger, D.J., and Singh, U. (2007) Trichostatin A effects on gene expression in the protozoan parasite *Entamoeba histolytica*. *BMC Genomics* **8:** 216.

Ellis, J.G., Davila, M., and Chakrabarti, R. (2003) Potential involvement of extracellular signal-regulated kinase 1 and 2 in encystation of a primitive eukaryote, *Giardia lamblia*. Stage-specific activation and intracellular localization. *J Biol Chem* **278:** 1936–1945.

Elmendorf, H.G., Singer, S.M., Pierce, J., Cowan, J., and Nash, T.E. (2001) Initiator and upstream elements in the alpha2-tubulin promoter of *Giardia lamblia*. *Mol Biochem Parasitol* **113:** 157–169.

Finnin, M.S., Donigian, J.R., Cohen, A., Richon, V.M., Rifkind, R.A., Marks, P.A., *et al.* (1999) Structures of a histone deacetylase homologue bound to the TSA and SAHA inhibitors. *Nature* **401:** 188–193.

Franzen, O., Jerlstrom-Hultqvist, J., Castro, E., Sherwood, E., Ankarklev, J., Reiner, D.S., *et al.* (2009) Draft genome sequencing of giardia intestinalis assemblage B isolate GS: is human giardiasis caused by two different species? *PLoS Pathog* **5:** e1000560.

Gerwig, G.J., van Kuik, J.A., Leeflang, B.R., Kamerling, J.P., Vliegenthart, J.F., Karr, C.D., and Jarroll, E.L. (2002) The *Giardia* intestinalis filamentous cyst wall contains a novel beta(1–3)-N-acetyl-D-galactosamine polymer: a structural and conformational study. *Glycobiology* **12:** 499–505.

Gillin, F.D., Boucher, S.E., Rossi, S.S., and Reiner, D.S. (1989) *Giardia lamblia*: the roles of bile, lactic acid, and pH in the completion of the life cycle in vitro. *Exp Parasitol* **69:** 164–174.

Glozak, M.A., and Seto, E. (2007) Histone deacetylases and cancer. *Oncogene* **26:** 5420–5432.

Guex, N., and Peitsch, M.C. (1997) SWISS-MODEL and the Swiss-PdbViewer: an environment for comparative protein modeling. *Electrophoresis* **18:** 2714–2723.

Haumaitre, C., Lenoir, O., and Scharfmann, R. (2009) Directing cell differentiation with small-molecule histone deacetylase inhibitors: the example of promoting pancreatic endocrine cells. *Cell Cycle* **8:** 536–544.

Hehl, A.B., and Marti, M. (2004) Secretory protein trafficking in *Giardia* intestinalis. *Mol Microbiol* **53:** 19–28.

Hehl, A.B., Marti, M., and Kohler, P. (2000) Stage-specific expression and targeting of cyst wall protein-green fluorescent protein chimeras in *Giardia*. *Mol Biol Cell* **11:** 1789–1800.

Heller, G., Schmidt, W.M., Ziegler, B., Holzer, S., Mullauer, L., Bilban, M., *et al.* (2008) Genome-wide transcriptional response to 5-aza-2′-deoxycytidine and trichostatin a in multiple myeloma cells. *Cancer Res* **68:** 44–54.

Huang, Y.C., Su, L.H., Lee, G.A., Chiu, P.W., Cho, C.C., Wu, J.Y., and Sun, C.H. (2008) Regulation of cyst wall protein promoters by Myb2 in *Giardia lamblia*. *J Biol Chem* **283:** 31021–31029.

Iyer, L.M., Anantharaman, V., Wolf, M.Y., and Aravind, L. (2008) Comparative genomics of transcription factors and chromatin proteins in parasitic protists and other eukaryotes. *Int J Parasitol* **38:** 1–31.

Jenuwein, T., and Allis, C.D. (2001) Translating the histone code. *Science* **293:** 1074–1080.

Jimenez-Garcia, L.F., Zavala, G., Chavez-Munguia, B., Ramos-Godinez Mdel, P., Lopez-Velazquez, G., Segura-Valdez Mde, L., *et al.* (2008) Identification of nucleoli in the early branching protist *Giardia duodenalis*. *Int J Parasitol* **38:** 1297–1304.

Knodler, L.A., Svard, S.G., Silberman, J.D., Davids, B.J., and Gillin, F.D. (1999) Developmental gene regulation in *Giardia lamblia*: first evidence for an encystation-specific promoter and differential 5′ mRNA processing. *Mol Microbiol* **34:** 327–340.

Kouzarides, T. (2007) Chromatin modifications and their function. *Cell* **128:** 693–705.

Kulakova, L., Singer, S.M., Conrad, J., and Nash, T.E. (2006) Epigenetic mechanisms are involved in the control of *Giardia lamblia* antigenic variation. *Mol Microbiol* **61:** 1533–1542.

Kurdistani, S.K., and Grunstein, M. (2003) Histone acetylation and deacetylation in yeast. *Nat Rev Mol Cell Biol* **4:** 276–284.

Lalle, M., Salzano, A.M., Crescenzi, M., and Pozio, E. (2006) The *Giardia duodenalis* 14–3-3 protein is post-translationally modified by phosphorylation and polyglycylation of the C-terminal tail. *J Biol Chem* **281:** 5137–5148.

Lauwaet, T., Davids, B.J., Torres-Escobar, A., Birkeland, S.R., Cipriano, M.J., Preheim, S.P., *et al.* (2007) Protein phosphatase 2A plays a crucial role in *Giardia lamblia* differentiation. *Mol Biochem Parasitol* **152:** 80–89.

Lujan, H.D., Mowatt, M.R., and Nash, T.E. (1998) The molecular mechanisms of giardia encystation. *Parasitol Today* **14:** 446–450.

Margueron, R., Trojer, P., and Reinberg, D. (2005) The key to development: interpreting the histone code? *Curr Opin Genet Dev* **15:** 163–176.

Marti, M., and Hehl, A.B. (2003) Encystation-specific vesicles in *Giardia*: a primordial Golgi or just another secretory compartment? *Trends Parasitol* **19:** 440–446.

Marti, M., Li, Y., Schraner, E.M., Wild, P., Kohler, P., and Hehl, A.B. (2003) The secretory apparatus of an ancient eukaryote: protein sorting to separate export pathways occurs before formation of transient Golgi-like compartments. *Mol Biol Cell* **14:** 1433–1447.

Monis, P.T., Caccio, S.M., and Thompson, R.C. (2009) Variation in *Giardia*: towards a taxonomic revision of the genus. *Trends Parasitol* **25:** 93–100.

Mori, H., Urano, Y., Abe, F., Furukawa, S., Tsurumi, Y., Sakamoto, K., *et al.* (2003) FR235222, a fungal metabolite, is a novel immunosuppressant that inhibits mammalian histone deacetylase (HDAC). I. Taxonomy, fermentation, isolation and biological activities. *J Antibiot (Tokyo)* **56:** 72–79.

Morrison, H.G., McArthur, A.G., Gillin, F.D., Aley, S.B., Adam, R.D., Olsen, G.J., *et al.* (2007) Genomic minimalism in the early diverging intestinal parasite *Giardia lamblia*. *Science* **317:** 1921–1926.

Pan, Y.J., Cho, C.C., Kao, Y.Y., and Sun, C.H. (2009) A Novel WRKY-like Protein Involved in Transcriptional Activation of Cyst Wall Protein Genes in *Giardia lamblia*. *J Biol Chem* **284:** 17975–17988.

Pflum, M.K., Tong, J.K., Lane, W.S., and Schreiber, S.L. (2001) Histone deacetylase 1 phosphorylation promotes enzymatic activity and complex formation. *J Biol Chem* **276:** 47733–47741.

Ramakrishnan, G., Gilchrist, C.A., Musa, H., Torok, M.S., Grant, P.A., Mann, B.J., and Petri, W.A., Jr (2004) Histone acetyltransferases and deacetylase in *Entamoeba histolytica*. *Mol Biochem Parasitol* **138:** 205–216.

Rehrauer, H., Zoller, S., and Schlapbach, R. (2007) MAGMA: analysis of two-channel microarrays made easy. *Nucleic Acids Res* **35:** W86–W90.

Rodriquez, M., Terracciano, S., Cini, E., Settembrini, G., Bruno, I., Bifulco, G., *et al.* (2006) Total synthesis, NMR solution structure, and binding model of the potent histone deacetylase inhibitor FR235222. *Angew Chem Int Ed Engl* **45:** 423–427.

Saksouk, N., Bhatti, M.M., Kieffer, S., Smith, A.T., Musset, K., Garin, J., *et al.* (2005) Histone-modifying complexes regulate gene expression pertinent to the differentiation of the protozoan parasite *Toxoplasma gondii*. *Mol Cell Biol* **25:** 10301–10314.

Schemies, J., Sippl, W., and Jung, M. (2009) Histone deacetylase inhibitors that target tubulin. *Cancer Lett* **280:** 222–232.

Schwede, T., Kopp, J., Guex, N., and Peitsch, M.C. (2003) SWISS-MODEL: an automated protein homology-modeling server. *Nucleic Acids Res* **31:** 3381–3385.

Smith, G.K. (2005) *Limma: Linear Models for Microarray Data*. New York: Springer.

Sonda, S., Stefanic, S., and Hehl, A.B. (2008) A sphingolipid inhibitor induces a cytokinesis arrest and blocks stage differentiation in *Giardia lamblia*. *Antimicrob Agents Chemother* **52:** 563–569.

Stefanic, S., Morf, L., Kulangara, C., Regos, A., Sonda, S., Schraner, E., *et al.* (2009) Neogenesis and maturation of transient Golgi-like cisternae in a simple eukaryote. *J Cell Sci* **122:** 2846–2856.

Sun, C.H., Palm, D., McArthur, A.G., Svard, S.G., and Gillin, F.D. (2002) A novel Myb-related protein involved in transcriptional activation of encystation genes in *Giardia lamblia*. *Mol Microbiol* **46:** 971–984.

Sun, C.H., Su, L.H., and Gillin, F.D. (2006) Novel plant-GARP-like transcription factors in *Giardia lamblia*. *Mol Biochem Parasitol* **146:** 45–57.

Touz, M.C., Nores, M.J., Slavin, I., Carmona, C., Conrad, J.T., Mowatt, M.R., *et al.* (2002a) The activity of a developmentally regulated cysteine proteinase is required for cyst wall formation in the primitive eukaryote *Giardia lamblia*. *J Biol Chem* **277:** 8474–8481.

Touz, M.C., Nores, M.J., Slavin, I., Piacenza, L., Acosta, D., Carmona, C., and Lujan, H.D. (2002b) Membrane-associated dipeptidyl peptidase IV is involved in encystation-specific gene expression during *Giardia* differentiation. *Biochem J* **364:** 703–710.

Touz, M.C., Ropolo, A.S., Rivero, M.R., Vranych, C.V., Conrad, J.T., Svard, S.G., and Nash, T.E. (2008) Arginine deiminase has multiple regulatory roles in the biology of *Giardia lamblia*. *J Cell Sci* **121:** 2930–2938.

Triana, O., Galanti, N., Olea, N., Hellman, U., Wernstedt, C., Lujan, H., *et al.* (2001) Chromatin and histones from *Giardia lamblia*: a new puzzle in primitive eukaryotes. *J Cell Biochem* **82:** 573–582.

Vannini, A., Volpari, C., Filocamo, G., Casavola, E.C., Brunetti, M., Renzoni, D., *et al.* (2004) Crystal structure of a eukaryotic zinc-dependent histone deacetylase, human HDAC8, complexed with a hydroxamic acid inhibitor. *Proc Natl Acad Sci USA* **101:** 15064–15069.

Vannini, A., Volpari, C., Gallinari, P., Jones, P., Mattu, M., Carfi, A., *et al.* (2007) Substrate binding to histone deacetylases as shown by the crystal structure of the HDAC8-substrate complex. *EMBO Rep* **8:** 879–884.

Wang, C.H., Su, L.H., and Sun, C.H. (2007) A novel ARID/Bright-like protein involved in transcriptional activation of cyst wall protein 1 gene in *Giardia lamblia*. *J Biol Chem* **282:** 8905–8914.

Supporting information

Additional supporting information may be found in the online version of this article.

Please note: Wiley-Blackwell are not responsible for the content or functionality of any supporting materials supplied by the authors. Any queries (other than missing material) should be directed to the corresponding author for the article.